Optimization and Characterization of Human Vascularized Adipose tissue Model

Maaria Palmroth
Master's Thesis
University of Tampere
BioMediTech
May 2015

Acknowledgements

This Master's thesis project was carried out at the Finnish Center for Alternative Methods, FICAM, which is run by Docent Tuula Heinonen, PhD. FICAM is located in the School of Medicine, at the University of Tampere. Firstly, I would like to thank Tuula for giving me the great opportunity to explore this really interesting field of science. In addition to *in vitro* tissue models, I have learned a lot about GLP.

I want to express my greatest gratitude to my supervisors Doctor Tarja Toimela, PhD, and Ms Outi Huttala, MSc, for all the guidance and help you gave me. Without your excellent know-how and support, conducting this project would have been impossible. In addition, I am very grateful to Ms Sari Leinonen, who introduced me to the hands-on laboratory work and gave me technical support in the lab.

I am grateful also to Ms Marika Mannerström, PhL, and Ms Maaret Vaani for introducing and guiding me in the world of GLP. I would also like to thank Ms Hanna Vuorenpää, MSc, and Ms Pauliina Salonen, MSc, for all the help and support you gave me during this project. I am grateful also to all of the rest of you working at FICAM. I really enjoyed getting to know you all and working with you.

I would also like to thank my family. You have always been there for me and supported me throughout my studies. Special thanks go to my parents Anne and Jouko. I am grateful also to all of my friends, who made my study years memorable. Last but not least, I want to thank Aleksi for all the love and support.

Tampere, May 2015

Maaria Palmroth

Pro gradu –tutkielma

Paikka: Tampereen yliopisto
BioMediTech
Tekijä: Palmroth, Maaria Helena
Otsikko: Ihmissolupohjaisen verisuonitetun rasvamallin optimointi ja karakterisointi
Sivumäärä: 64 s. + liitteet 2 s.
Ohjaajat: FT Tarja Toimela, FM Outi Huttala
Tarkastajat: Professori Markku Kulomaa, FT Tarja Toimela
Päiväys: Toukokuu 2015

Tiivistelmä

Tutkimuksen tausta ja tavoitteet: Monet rasvakudokseen liittyvät sairaudet, kuten esimerkiksi sairaalloinen lihavuus ja tyypin 2 diabetes, ovat jo saavuttaneet maailmanlaajuisten epidemioiden mittasuhteet. Rasvakudos toimii kehossa energiavarastona. Tämän lisäksi rasvakudos on merkittävä endokriininen elin, joka on erityisen tiiviissä yhteydessä verisuonistoon. Rasvakudoksen ja sen sairauksien tutkimukseen on kehitetty paljon erilaisia eläinmalleja. Eläinmalleilla saavutetut tulokset eivät kuitenkaan vastaa hyvin tilannetta ihmisessä, minkä vuoksi tarvitaan uusia ja tarkempia ihmissolupohjaisia kudosmalleja. Tämän tutkimuksen tavoitteena oli optimoida ja karakterisoida ihmissolupohjainen verisuonitettu rasvamalli. Tutkimuksessa määritettiin, vaikuttaako verisuonten lisääminen rasvamalliin positiivisesti rasvan kypsymiseen, muodostuuko malliin kunnollisia verisuoniverkostoja rasvasolujen läsnä ollessa ja voidaanko solujen irtoamisongelma ratkaista vaihtamalla solujen siirrostus- ja erilaistusstrategiaa.

Tutkimusmenetelmät: Tutkimuksessa mallinnettiin verisuonitetun rasvakudoksen muodostumista viljelemällä ihmisen rasvan kantasoluja ja ihmisen napanuoran endoteelisoluja yhteisviljelmässä 14 päivää. Työssä kokeiltiin kuutta erilaista siirrostus- ja erilaistusstrategiaa. Yhteisviljelmää käsiteltiin viljelyn aikana sekä rasva- että verisuonierilaistusmediumeilla. Viljelyn päätyttyä, triglyseridien kertymistä tutkittiin Adipored reagenssilla, solujen suhteellista määrää WST-1 reagenssilla ja verisuonten muodostumista immunosytokemiallisilla värjäyksillä. Rasvakudosspesifien geenien ilmentymistä tutkittiin RT-qPCR -menetelmällä soluviljelyn 14. päivänä. Triglyseridien kertymistä ja verisuonten muodostumista havainnoitiin fluoresenssimikroskoopilla. Muodostuneita verisuonia tutkittiin myös konfokaalimikroskoopilla sekä Cell-IQ -laitteella. Myös verisuonten pinta-ala määritettiin.

Tulokset: Soluviljelystrategia, jossa rasvakudos erilaistettiin ennen verisuonia, ja jossa solut siirrostettiin kahdessa erässä kahtena eri päivänä, oli teknisesti paras strategia ratkaisemaan solujen irtoamisongelman, kerrytti triglyseridejä riittävissä määrin, ilmensi rasvakudosspesifisiä geenejä ja muodosti rasvasoluja ja verisuonia, jotka olivat morfologialtaan samankaltaisia kuin rasvasolut ja verisuonet *in vivo.*

Johtopäätökset: Tulokset osoittivat, että solujen erilaisilla siirrostus- ja erilaistusstrategioilla oli merkitystä mallin tekniseen toteuttamiseen ja toistettavuuteen, triglyseridien kertymiseen, verisuonirakenteiden muodostumiseen ja muodostuneen rasvakudoksen geneettiseen kypsyyteen. Verisuonitettu rasvamalli on lupaava työkalu rasvakudoksen tutkimiseen. Kudosmallin perusteellisella karakterisoinnilla ja optimoinnilla on mahdollista luoda nykyisin saatavilla olevia eläinmalleja tehokkaampi, tarkempi ja luotettavampi testisysteemi.

Master's Thesis

Place: University of Tampere
BioMediTech
Author: Palmroth, Maaria Helena
Title: Optimization and characterization of human vascularized adipose tissue model
Pages: 64 pp. + appendices 2 pp.
Supervisors: Dr Tarja Toimela, PhD, Ms Outi Huttala, MSc
Reviewers: Professor Markku Kulomaa, PhD, Dr Tarja Toimela, PhD
Date: May 2015

Abstract

Background and aims: Many adipose tissue related diseases, such as obesity and type 2 diabetes, are already worldwide epidemics. In addition to being energy storage, adipose tissue is an endocrine organ, which is in particular closely associated with vascular system. In order to study adipose tissue and diseases related to it, a wide variety of animal models have been developed. However, the results obtained with these models correlate relatively poorly to humans. Thus, new and more accurate human cell based models are needed. The aim of this study was the optimization and characterization of human vascularized adipose tissue model. The more specific aims were to determine whether adding tubules to adipose tissue model would have a positive effect on the maturation of adipocytes, whether proper vascular structures are formed in the model in the presence of adipocytes and, whether the problem of cell detachment can be solved by trying different cell plating and differentiation schemes.

Methods: Human adipose stromal cells (hASC) and human umbilical cord vein endothelial cells (HUVEC) were cultured as a co-culture on a 48-well plate to mimic vascularized adipose tissue *in vitro*. Six different cell culturing strategies with respect to cell plating and differentiation schemes were tested. Co-cultures were grown for 14 days and during the co-culture, exposed both to adipogenic and angiogenic differentiation media. After this, triglyceride accumulation was studied with Adipored reagent, the relative cell number with WST-1 reagent and the formed vascular structures with immunocytochemical stainings. Adipocyte specific gene expression was studied with RT-qPCR on the 14th day of cell culture. Triglyceride accumulation and vascular structure formation were observed with a fluorescent microscope. Vascular structures were also studied with confocal microscope and Cell-IQ and the area of vascular networks was quantified.

Results: The cell culturing scheme, in which adipogenesis was induced before angiogenesis, and where cells were plated in two batches at two different days, was the best cell culturing strategy for solving the detachment issue, accumulated triglycerides, expressed adipose tissue specific genes and the morphology of adipocytes and blood vessels was similar to their morphology *in vivo*.

Conclusions: The results showed, that changing cell plating and differentiation scheme affected the technical repeatability of the model, triglyceride accumulation, vascular structure formation and the genetic maturity of the formed adipose tissue. The vascularized adipose tissue model is a promising tool for adipose tissue research. By thorough characterizing and optimizing the developed *in vitro* model, it is possible to create a more efficient, reliable and accurate test method than the currently available animal models offer.

Table of Contents

Abbreviations

36B4	Acidic ribosomal phosphoprotein P0
Ang	Angiopoietin
AP2	Adipocyte lipid binding protein 2
ATE	Adipose tissue extract
ATGL	Adipose triglyceride lipase
BAT	Brown adipose tissue
BMSC	Bone-marrow-derived stem cell
BSA	Bovine serum albumin
cAMP	Cyclic adenosine monophosphate
C/EBPs	CCAAT/enhancer binding proteins
Col	Collagen
CO_2	Carbon dioxide
C_T	Cycle threshold
DEX	Dexamethasone
DMEM/F-12	Dulbecco's modified Eagle's medium Nutrient Mixture F-12
(D)PBS	(Dulbecco's) Phosphate buffer saline
EC	Endothelial cell
ECM	Extracellular matrix
ES	Embryonic stem cells
FGF	Fibroblast growth factor
Glut4	Glucose transporter 4
hASC	Human adipose stromal cell
HFD	High-fat diet
HGF	Hepatocyte growth factor
HSL	Hormone-sensitive lipase
HUVEC	Human umbilical cord vein endothelial cell
IBMX	Isobuthylmethylxanthine
IL-6	Interleukin 6
IGF	Insulin-like growth factor
LPL	Lipoprotein lipase
MGL	Monoglyceride lipase
MEK/ERK	Mitogen-activated protein kinase kinase/extracellular signal regulated kinase
MMPs	Matrix metalloproteinases
p38 MAPK	P38 mitogen-activated protein kinase
PAI-I	Plasminogen activator inhibitor-1
PDGF	Platelet derived growth factor
PKA	Protein kinase A
PKC	Protein kinase C
PIGF	Placental growth factor
PPARγ	Peroxisome proliferator-activated receptor γ
SDHA	Succinate dehydrogenase complex, subunit A
SVF	Stromal vascular fraction
TGF	Transforming growth factor
TIMPs	Tissue inhibitors of matrix metalloproteinases
TNFα	Tumor necrosis factor-alpha
VEGF	Vascular endothelial growth factor
VLDL	Very-low-density lipoprotein
WAT	White adipose tissue

1. Introduction

The prevalence of several adipose tissue related diseases, such as obesity and type 2 diabetes, have reached worldwide epidemic proportions. Already 2.1 billion people are obese and over 371 million people have type 2 diabetes (Lai et al., 2014). In addition to type 2 diabetes, obesity and overweight are associated with an increased incidence of other comorbidities including several different cancer types, sleep apnea, asthma, degenerative joint disease, hypertension, renal failure, stroke, and cardiovascular disease (Switzer et al., 2013; van Baak, 2013).

Adipose tissue is a complex organ that has many important functions in the body. In addition to adipocytes, adipose tissue contains stromal-vascular cells, blood vessels, lymph nodes and nerves (J. H. Choi et al., 2010). For a long time adipose tissue was considered merely as energy storage, but nowadays it is clear that adipose tissue does a lot more. It is a dynamic endocrine organ secreting many different bioactive factors that control systemic insulin sensitivity, energy metabolism, immune responses and cardiovascular homeostasis (Gu & Xu, 2013). Adipose tissue serves also as a mechanical support for the body and insulates heat (Rosen & Spiegelman, 2014).

Adipose tissue is particularly intimately associated to the vascular system, being one of the most vascularized tissues in the body (Y. Cao, 2013). Adipose tissue secretes both pro- and anti-angiogenic factors and the vascular system supports the growth and function of adipose tissue (Y. Cao, 2014, Christiaens & Lijnen, 2010). The vascular system does not only bring oxygen, nutrients, cytokines, growth factors and stem cells to adipose tissue and remove waste products from adipose tissue through circulation but also produces local growth factors and cytokines that communicate with adipose tissue (Y. Cao, 2014). In addition, vascular pericytes have been noticed to have stem cell features and can differentiate into preadipocytes and adipocytes (Tran et al., 2012). Thus, adipose tissue expansion could be controlled through angiogenesis prevention, which has led to new experimental obesity treatments (Y. Cao, 2013; Daquinag et al., 2011).

A wide variety of animal models have been generated in order to study obesity. The species used include fruit flies, dogs, cats, pigs, rabbits, hamsters, squirrels, mice, rats and primates (Lai et al., 2014). However, the results obtained with animal models translate relatively

poorly to humans (Bergen & Mersmann, 2005; Chandrasekera & Pippin, 2014; Lai et al., 2014). The complex pathways of lipid metabolism are mostly species specific (Bergen & Mersmann, 2005). There are also ethical aspects related to animal studies (Sade, 2011). Thus, new human cell based methods offer biologically relevant tools for the study of human adipose tissue related diseases. Development of *in vitro* adipose tissue models is also interesting from a tissue-engineering point of view (Kang et al., 2009). Soft tissue reconstruction is often needed, when a patient loses soft tissue due to injury, trauma or disease (J. H. Choi et al., 2010). In addition to the cosmetic and emotional well-being of the patient, the loss of adipose tissue can impair function, such as range of motion (Patrick, 2001).

In this study, human adipogenesis and angiogenesis cell models developed earlier at FICAM (Huttala et al., 2015; Sarkanen et al., 2012a; Sarkanen et al., 2012b) were combined to form a functional vascularized adipose tissue model. Different cell culturing strategies for building the model were examined, in order to find out how they affect the maturation of the adipose tissue, the formation of vascular networks and the technical repeatability and reliability of the model.

2. Literature review

2.1 Adipose tissue

Adipose tissue is typically divided into two major types, white adipose tissue (WAT) and brown adipose tissue (BAT). White adipocytes store lipids in one, large lipid droplet, while brown adipocytes contain several smaller lipid droplets (Hyvonen & Spalding, 2014; Peirce et al., 2014). BAT is present mainly in infants and it is responsible for the non-shivering thermogenesis, where triglycerides are oxidized for heat production (J. H. Choi et al., 2010; Hyvonen & Spalding, 2014). The amount of BAT decreases in humans as the body matures, while the amount of WAT increases (J. H. Choi et al., 2010).

WAT is highly dynamic tissue, as it can rapidly respond to the changes in the energy balance of the body by increasing or decreasing its mass (Hyvonen & Spalding, 2014; Sun et al., 2011). WAT is distributed all over the body and can be classified by type and depot: the subcutaneous (e.g. arm, abdominal and gluteal adipose tissue), the intraabdominal (e.g. visceral) and other sites (e.g. intramuscular) (J. H. Choi et al., 2010). WAT in different depots differs from each other (Hyvonen & Spalding, 2014; Rosen & Spiegelman, 2014). For example, increased amount of visceral fat is known to raise the risk of the metabolic syndrome whereas increased amount of subcutaneous fat does not or might even decrease the risk (Hyvonen & Spalding, 2014; Rosen & Spiegelman, 2014).

Mature adipocytes constitute the majority of WAT. However, they account for 20 - 60 % of the total cell number in WAT (Hyvonen & Spalding, 2014; Lanthier & Leclercq, 2014). In addition to mature adipocytes, WAT contains stromal vascular fraction cells (SVF cells), which are a heterogeneous group of cells including endothelial cells, macrophages, fibroblasts, stem cells and lymphocytes (J. H. Choi et al., 2010; Hyvonen & Spalding, 2014). WAT is highly vascularized tissue and contains an extensive system of lymph nodes and nerves (Y. Cao, 2013; J. H. Choi et al., 2010). WAT is supported by the extracellular matrix (ECM), which consists of collagen types I, III, IV, V and VI in addition to other ECM proteins (J. H. Choi et al., 2010).

Quite recently, a third type of adipocyte has been discovered. These cells are typically referred to brite cells, for their brown-in-white phenotype (also known as beige, inducible, recruitable, brown-like or paucilocular cells) (Hyvonen & Spalding, 2014; Peirce et al., 2014). Brite cells are interspersed among WAT, where they are capable of thermogenesis (Hyvonen

& Spalding, 2014; Peirce et al., 2014). Although there is a rising interest in the metabolism and function of BAT (J. H. Choi et al., 2010) and BAT/brite cell activation might offer new therapeutic targets for treating metabolic diseases (Harms & Seale, 2013), this thesis focuses on WAT, as it is the major form of adipose tissue in humans and as the cells used in this study are obtained from WAT.

2.2 Adipogenesis

The development of adipose tissue compartments begins at late gestation (Cristancho & Lazar, 2011). The rate of adipogenesis emerges in response to increased nutrient availability that leads to the remarkable postnatal expansion of adipose tissue (Cristancho & Lazar, 2011). Expansion of adipose tissue after birth occurs both by the increment of adipocyte size and adipocyte number (Gregoire et al., 1998). It seems that the expansion of adipose tissue can occur by both ways also in the adult stage, but the relative contribution of adipocyte size and adipocyte number to human adipose tissue growth in response to nutritional stimulus remains unclear (Cristancho & Lazar, 2011; Gregoire et al., 1998).

Adipogenesis is typically described as a two-phase process that includes determination (also known as commitment) and terminal differentiation (Cristancho & Lazar, 2011; Rosen & MacDougald, 2006). In the determination phase, stem cells transform into committed preadipocytes (Rosen & MacDougald, 2006). These preadipocytes cannot differentiate anymore into other cell types than adipocytes (Rosen & MacDougald, 2006). However, before further differentiation, the growth arrest of preadipocytes is required (Gregoire, 2001). Following growth arrest, preadipocytes need also an appropriate mixture of adipogenic and mitogenic signals for terminal differentiation (Gregoire, 2001).

In terminal differentiation, preadipocytes transform into insulin-sensitive, lipid synthesizing and transporting mature adipocytes that secrete adipocyte-specific secretory products (Gregoire et al., 1998; Rosen & MacDougald, 2006). Adipocyte differentiation into mature adipocyte phenotype is typically characterized by chronological changes in the expression of multiple genes (Gregoire et al., 1998). The changes can be detected by the early, intermediate and late mRNA/protein markers and triglyceride accumulation (Gregoire et al., 1998). A schematic picture of adipogenesis is represented in Figure 1.

2.2.1 The molecular events and regulation of adipogenesis

Adipogenesis requires the coordinated activation of over 2000 genes (Gregoire, 2001). The most important transcriptional factors include peroxisome proliferator-activated receptor γ

(PPARγ) and CCAAT/enhancer binding proteins (C/EBPs) (Bucky & Percec, 2008; Gregoire, 2001; Rosen & MacDougald, 2006).

PPARγ is often referred to the 'master regulator' of adipogenesis. PPARγ belongs to nuclear-receptor superfamily and its expression alone is sufficient for adipocyte differentiation (Farmer, 2006; Rosen & MacDougald, 2006). In the absence of PPARγ, no other transcription factor can promote adipocyte differentiation (Rosen & MacDougald, 2006). Moreover, most pro-adipogenic factors operate by the activation of PPARγ expression or activity (Rosen & MacDougald, 2006). Due to alternative promoter usage and splicing, PPARγ is expressed as two different isoforms, PPARγ1 and PPARγ2. During adipogenesis, both isoforms are expressed, but PPARγ2 is exclusively expressed in adipose tissue whereas PPARγ1 is expressed also in other tissues besides adipose tissue (Farmer, 2006; Rosen & MacDougald, 2006). The relative roles of two different isoforms remain inconclusive, as it seems that although PPARγ2 might be essential for obtaining the insulin sensitivity of adipocytes, it is not absolutely necessary for adipocyte differentiation, when PPARγ1 is expressed (Rosen & MacDougald, 2006). PPARγ is not only vital for adipocyte differentiation, but it is also needed for the regulation of insulin sensitivity, lipogenesis and adipocyte survival and function (Lefterova et al., 2014).

C/EBPs (α, β and δ) are important activators of PPARγ. C/EBP-β and C/EBP-δ stimulate the expression of PPARγ in early differentiation (Bucky & Percec, 2008; Rosen & MacDougald, 2006). PPARγ and C/EBP-β activate then C/EBP-α, which induces many adipogenic genes directly and activates PPARγ (Rosen & MacDougald, 2006). The activation of C/EBP-α induced by PPARγ creates a positive feedback signal that maintains the differentiated adipogenic state (Daquinag et al., 2011).

In addition to PPARγ and C/EBPs, many other transcriptional factors effect on adipogenesis. For example, ADD1/SREBP-1c, CREB, Krüppel-like factors (KLF5, KLF15, and KLF2), early growth response 2, early B-cell factors and lipoprotein lipase (LPL) have been discovered to be important inducers of adipogenesis (Bucky & Percec, 2008; Gregoire et al., 1998). Also factors of negative regulation have been discovered: GATA binding transcription factors GATA-2 and GATA-3 function as anti-adipogenic transcriptional factors (Gregoire, 2001; Rosen & MacDougald, 2006).

Besides transcriptional factors, also other signaling molecules participate in the regulation of adipogenesis. Among other pathways, the activation of mitogen-activated protein kinase

kinase/extracellular signal regulated kinase (MEK/ERK) signaling pathway and p38 mitogen-activated protein kinase (p38 MAPK) signaling pathway are required for adipogenesis (Bost et al., 2005; Farmer, 2005). Also insulin, insulin-like growth factor 1 (IGF-1), glucocorticoids and agents that increase intracellular cyclic adenosine monophosphate (cAMP) concentrations act as promoters of adipogenesis (Gregoire et al., 1998), whereas Wnt family, pref-1, transforming growth-factor β (TGF-β) superfamily members, cytokines and protein kinase C (PKC) are inhibitory extracellular signal molecules of adipogenesis (Gregoire, 2001; Rosen & MacDougald, 2006).

Furthermore, one of the key regulators of the adipocyte differentiation is the shape transformation of fibroblast-like shaped preadipocytes into more spherical shaped preadipocytes (Gregoire, 2001). These morphological modifications are correspondent to the changes in ECM and promote the expression of C/EBPα and/or PPARγ (Gregoire, 2001). In addition to cell-shape change, the modification of ECM is needed for adipocyte-specific gene expression and lipid accumulation (Selvarajan et al., 2001).

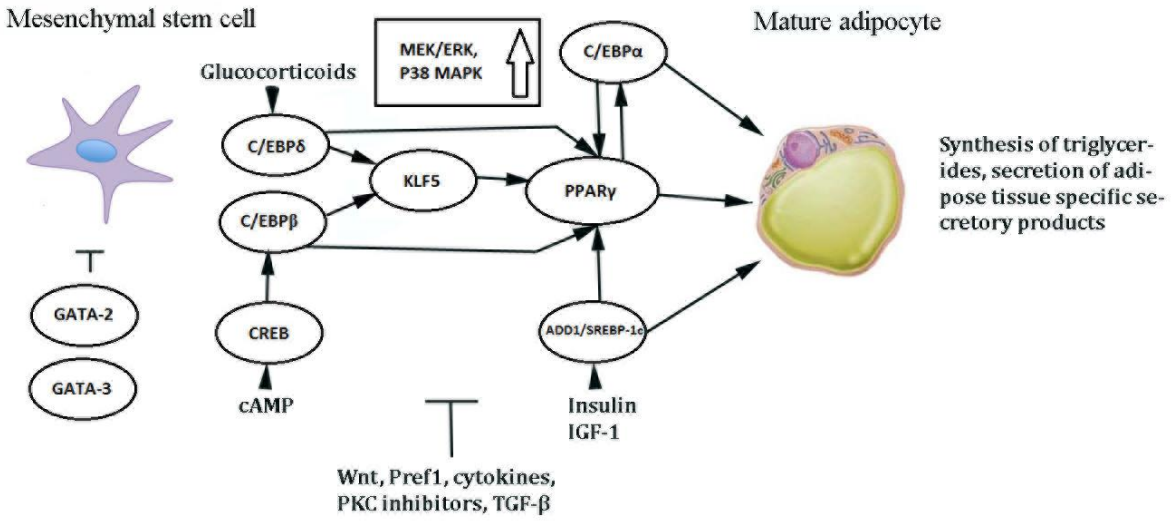

Figure 1: The key regulators of adipogenesis. C/EBPδ and C/EBPβ stimulate KLF5 and PPARγ in the early differentiation. PPARγ is the most important transcriptional regulator of adipogenesis and is further activated by ADD1/SREBP-1c. C/EBPβ and PPARγ activate C/EBPα, which activates PPARγ creating a positive feedback-signal to maintain the differentiated state. GATA-2 and GATA-3 act as inhibitory transcriptional factors. Glucocorticoids, cAMP, insulin and IGF-1 stimulate adipogenesis, whereas Wnt, Pref1, cytokines, PKC inhibitors and TGF-β inhibit adipogenesis. During adipogenesis, MEK/ERK and p38 MAPK signaling pathways are activated.

2.3 Adipocyte metabolism

2.3.1 Lipid metabolism in adipocytes

Triglycerides (triacylglycerides) are the major storage molecules for fatty acids for energy utilization and for the synthesis material of membrane lipids (Yen et al., 2008). Triglycerides are stored in cells in lipid droplets, which can be found in most cell types in vertebrates (Brasaemle & Wolins, 2012; Walther & Farese, 2012). However, adipocytes are the only cell type that is specialized in lipid storage: while lipid droplets in other cell types have the diameters of 100 - 200 nm, lipid droplets in adipocytes have diameters up to 100 µm and fill almost the whole cytoplasm (Walther & Farese, 2012).

Triglycerides are transported in the circulation in the form of multi-molecular lipoprotein particles (Mead et al., 2002). Dietary triglycerides are packed into chylomicrone lipoproteins by the intestine, whereas triglycerides synthetized in the liver are packed into very-low-density lipoprotein (VLDL) particles (Kersten, 2014; Mead et al., 2002). Adipocytes, as well as some other cell types, utilize circulating triglycerides with the help of lipoprotein lipase (LPL) (Frayn et al., 2003; Kersten, 2014). As adipocytes release LPL, LPL is transported to the lumenal side of capillary endothelium (Kersten, 2014). Then, LPL catalyzes the hydrolysis of circulating chylomicrons and VLDL (Mead et al., 2002). This reaction provides non-esterified fatty acids and 2-monoacylglycerols (Mead et al., 2002; Rutkowski et al., 2015). Non-esterified fatty acids are taken into adipocytes by several binding and transport proteins, such as CD36 and fatty acid transport protein family (Rutkowski et al., 2015). Upon transportation into adipocytes, non-esterified fatty acids are esterified to a glycerol backbone (Mead et al., 2002; Rutkowski et al., 2015). Esterification thus forms triglycerides for storage within the lipid droplets in adipocytes (Rutkowski et al., 2015). Adipocytes are also capable of *de novo* lipogenesis and can take in free fatty acids in the fasting state (Hames et al., 2015; Rosen & Spiegelman, 2014).

Fatty acids are released from triglycerides, so that they can be oxidized locally or by other organs, through the process called lipolysis (Rosen & Spiegelman, 2014; Rutkowski et al., 2015). The surface of lipid droplets includes structural proteins and metabolic enzymes that are specified to adipocytes and respond to hormonal stimulation of lipolysis (Rutkowski et al., 2015). Lipolysis is classically thought to be driven by β-adrenergic signaling in adipocytes, but it is possible that also other inducers can stimulate lipolysis (Rosen & Spiegelman, 2014). The binding of cathecolamins to β-adrenergic receptors results in the increased concentration of cellular cyclic adenosine monophosphate (cAMP), which in turn activates lipolytic

enzymes through the stimulation of protein kinase A (PKA) (Zechner et al., 2005). Lipolytic enzymes include at least three major enzymes: adipose triglyceride lipase (ATGL), hormone-sensitive lipase (HSL) and monoglyceride lipase (MGL) (Rosen & Spiegelman, 2014). ATGL functions as the initiator of triglyceride hydrolysis and results in the generation of diacylglycerols and free fatty acids (Zechner et al., 2005), while HSL functions as a diglyceride lipase and MGL completes the process by generating glycerol and free fatty acids (Rosen & Spiegelman, 2014).

2.3.2 Insulin action on adipocytes

Insulin is an important regulator of adipocyte metabolism. It promotes the synthesis and storage of triglycerides and inhibits their catabolism (Rutkowski et al., 2015). In the high fed state, insulin binds to its receptor on adipocytes and causes the translocation of glucose transporter 4 (Glut4) from the cytosol to the cell surface (Watson & Pessin, 2007). The translocation of Glut4 then enables effective glucose influx into the adipocytes (Watson & Pessin, 2007). Insulin-stimulated Glut4 seems to be the predominant glucose transporter type in adipocytes, although another glucose transporter type, Glut1, is constitutive present at the cell membranes of adipocytes (Rutkowski et al., 2015). Studies with adipocyte-specific Glut4 knock-out mice have shown that Glut4 deletion in adipocytes causes skeletal and hepatic insulin resistance, suggesting that adipocyte Glut4 - mediated glucose uptake plays an important role in glucose homeostasis (Abel et al., 2001). The influx of glucose is not just necessary for ATP production, as glucose is also needed for effective adipocyte lipid packaging (Guan et al., 2002).

Insulin acts also as a lipolysis inhibitor by activating phosphodiesterase 3B, which inactivates the function of cAMP (S. M. Choi et al., 2010). Thus, the downstream activation of PKA is inhibited as well as the activation of ATGL and HSL (S. M. Choi et al., 2010). Insulin inhibits lipolysis also indirectly by enhancing the influx of glucose (Rutkowski et al., 2015). Glucose is metabolized into pyruvate, which enters the citric acid cycle. However, a portion of pyruvate is metabolized into lactate. As lactate exits adipocytes, it mediates insulin-dependent inhibition through an autocrine and paracrine lactate loop (Ahmed et al., 2010). Lactate binding to the G protein-coupled receptor GPR81 inhibits the formation of cAMP and also the down-stream activation of PKA (Ahmed et al., 2010).

2.4 Adipose tissue secretory products

Adipose tissue is the largest endocrine organ of the human body (Burke et al., 2014). Mature adipose tissue secretes several hormones, growth factors, enzymes, matrix proteins, cytokines

and complement factors (Coelho et al., 2013; Poulos et al., 2010). The secreted factors regulate fat mass, adipogenesis, vasculature, blood flow, lipid and cholesterol metabolism and the function of the immune system (Poulos et al., 2010). In addition to adipose tissue and vasculature, the main organ systems affected by adipose tissue secretory products are liver, muscle, the brain, pancreatic β-cells and the reproductive track (Scherer, 2006). The most important adipose tissue secretory products are discussed in detail below and more secretory products and their main functions are listed in Table 1.

2.4.1 Adipose-derived hormones

Leptin and adiponectin are the most abundant hormones produced by adipose tissue (Coelho et al., 2013). They both regulate the whole body energy homeostasis via hypothalamus, albeit having opposite functions (Coelho et al., 2013; Galic et al., 2010). In addition, they have metabolic effects on other tissues (Galic et al., 2010).

2.4.1.1 Leptin

Leptin is the gene product of the obese gene and it is mainly produced and secreted by mature adipocytes (Gregoire, 2001). The main function of this peptide hormone is the regulation of the energy balance of the body (Coelho et al., 2013; Gregoire, 2001; Kershaw & Flier, 2004). The effects on the energy balance of leptin are mostly mediated by receptors located in the central nervous system, whereas other effects are mediated by receptors located in peripheral tissues, including muscle and pancreatic β-cells (Kershaw & Flier, 2004).

Adipose tissue and circulating leptin concentrations are dependent on the energy stored as fat and the current status of energy balance (Coelho et al., 2013; Rasouli & Kern, 2008). Thus, leptin concentrations are higher in obese individuals and increase with overfeeding (Coelho et al., 2013). Correspondingly, leptin concentrations decrease, when caloric intake is restricted and weight-loss occurs. This decrease in leptin concentration is associated with adaptive physiological responses to starvation, which include increased appetite and decreased energy expenditure (Kershaw & Flier, 2004). The absence of leptin or a mutation in leptin receptor leads to increased appetite and therefore to massive obesity, but the prevalence of these mutations in humans is rare (Coelho et al., 2013).

In addition to energy homeostasis regulation, leptin has other versatile effects on several tissues. It regulates neuro- and traditional endocrine systems, the immune system, hematopoiesis, angiogenesis and bone development (Kershaw & Flier, 2004).

2.4.1.2 Adiponectin

Adiponectin (also known as Arcp30, AdipoQ, apM1, and GBP28) is a full-length protein, which can circulate as homotrimer, higher molecular weight hexamer or as high molecular weight multimer (Coelho et al., 2013; Poulos et al., 2010). In addition, a fragment containing the globular domain of adiponectin circulates in the blood stream and shows metabolic activity in several tissues (Coelho et al., 2013; Kershaw & Flier, 2004). Adiponectin is secreted exclusively by adipose tissue (Kershaw & Flier, 2004). Two different adiponectin receptors have been discovered, adipoR1 and adipoR2 (Kershaw & Flier, 2004). Both of these receptor types are highly expressed in skeletal muscles (Coelho et al., 2013). AdipoR2 is also abundant in liver (Coelho et al., 2013; Kershaw & Flier, 2004).

Adiponectin regulates the energy balance of the body via activation of AMP-activated protein kinase in the hypothalamus (Coelho et al., 2013). Adiponectin stimulates appetite and reduces energy expenditure and thus has opposite functions compared with leptin (Coelho et al., 2013). In addition, adiponectin affects liver enhancing insulin sensitivity, increasing fatty acid oxidation, reducing hepatic glucose production and decreasing the influx of non-essential fatty acids (Kershaw & Flier, 2004). In muscles, adiponectin stimulates fatty acid oxidation and glucose intake (Kershaw & Flier, 2004).

2.4.2 Adipokines

Cytokines are peptides, which are produced as a respond to certain stimulation and are bioactive at very low concentrations (Thalmann & Meier, 2007). They have a central role in the regulation of inflammation, immunity, cell growth and maturation (Thalmann & Meier, 2007). Adipokines are cytokines produced by adipose tissue (Poulos et al., 2010). Thus far, numerous adipokines, such as chemerin, several interleukins, plasminogen activator inhibitor-1 (PAI-I), retinol binding protein 4, tumor necrosis factor-alpha (TNFα), interferons, tissue inhibitor of metalloproteinases 1 (TIMP-1) and visfatin has been discovered (Poulos et al., 2010).

The concentrations of pro-inflammatory adipokines, such as TNFα, IL-6 and PAI-I, are higher in obese individuals compared with lean individuals (Weisberg et al., 2003). These adipokines are mostly produced by SVF cells of adipose tissue (Weisberg et al., 2003). TNFα impairs insulin signaling in liver and in adipose tissue and can also reduce fatty-acid oxidation in liver and muscle (Galic et al., 2010). The increased levels of TNFα in obese individuals result from the increased infiltration of M1 macrophages into adipose tissue (Weisberg et al., 2003).

In addition to obesity, high IL-6 concentrations are associated with type 2 diabetes and hyperlipidemia (Galic et al., 2010; Kershaw & Flier, 2004). IL-6 has been demonstrated to impair insulin signaling in peripheral tissues by repressing the expression of insulin receptor components and inducing suppressor of cytokine signaling 3, which is a negative regulator of both insulin and leptin (Kershaw & Flier, 2004).

PAI-I acts in many biological processes, including angiogenesis, atherosgenesis and the regulation of thrombus formation by inhibiting fibrinolysis (Kershaw & Flier, 2004; Ronti et al., 2006). Elevated levels of PAI-I in plasma are associated with insulin resistance and predict the future risk of the metabolic syndrome, type 2 diabetes and cardiovascular disease (Kershaw & Flier, 2004). Thus, PAI-I is likely to contribute to the insulin resistance development in obesity and to connect obesity to cardiovascular disease (Kershaw & Flier, 2004).

2.4.3 Growth factors

Adipose tissue growth factors are typically considered as proteins that stimulate the proliferation and differentiation of cells. They can act either as endocrine hormones via blood stream or as paracrine manner to neighboring cells (Poulos et al., 2010).

Adipose tissue secretes several growth factors including insulin-like growth factor 1 (IGF-1), fibroblast growth factors (FGFs), transforming growth factors α and β (TGFα and TGFβ), vascular endothelial growth factors (VEGFs), hepatocyte growth factor (HGF), placental growth factor (PIGF), angiopoietin 1 and 2 (Ang-1 and Ang-2) and platelet derived growth factors (PDGFs) (Christiaens & Lijnen, 2010; Poulos et al., 2010).

The most important angiogenic growth factors secreted by adipose tissue are VEGF-A and HGF (Christiaens & Lijnen, 2010). Also FGF-2, TGFβ, VEGF-B, VEGF-C, PIGF, PDGFβ, Ang-1, Ang-2 have positive effects on angiogenesis (Christiaens & Lijnen, 2010). VEGFs are needed for the initiation of the immature blood vessel formation both in vasculogenesis and angiogenesis (G. J. Hausman & Richardson, 2004). VEGF-A and its receptors are the key regulators of endothelial cell proliferation and migration and it is believed to have the main responsibility of the angiogenic capacity of adipose tissue (Christiaens & Lijnen, 2010; G. J. Hausman & Richardson, 2004).

HGF is a multifunctional growth factor that promotes mitogenic and morphogenic activities during development and in several other biological processes (Christiaens & Lijnen, 2010). HGF has been discovered to promote the tube formation of human umbilical cord vein

endothelial cells (HUVECs) *in vitro* and is one of the key regulators of angiogenesis in developing adipose tissue (Bell et al., 2008; Saiki et al., 2006).

FGF-2 enhances the differentiation, proliferation and migration of human adipose-derived stem cells *in vitro* (Christiaens & Lijnen, 2010; Poulos et al., 2010). In addition, FGF-2 stimulates the synthesis of proteinases, such as collagenase and urokinase type plasminogen-activator during angiogenesis (Christiaens & Lijnen, 2010). TGFβ is a known inhibitor of mesenchymal cell differentiation into several cell types, including adipocytes (Poulos et al., 2010). TGFβ is also thought to be an important regulator of angiogenesis, as it regulates PAI-I production, release and transcription (Poulos et al., 2010).

2.4.4 Extracellular matrix components and enzymes

Adipose tissue contains a dense network of ECM, where every adipocyte is surrounded by basal lamina (Mariman & Wang, 2010; Sun et al., 2011). The major component of adipose tissue basal lamina is collagen VI (Divoux & Clement, 2011).

Adipocytes secrete a number of ECM components, especially collagen I, III, IV and VI (P. Wang et al., 2008). In addition, enzymes involved in ECM modification, such as ADAMTS (a disintegrin and metalloproteinase with thrombospondin motifs), MMPs (matrix metalloproteinases) and TIMPs (tissue inhibitors of MMPs) are expressed in adipose tissue (Mariman & Wang, 2010; Sun et al., 2011).

Members of ADAMTS family have been proven to have procollagen proteinase activity and they may also function in adipose tissue growth, as the expression of different family members change during the development of diet induced obesity (Mariman & Wang, 2010). MMPs are neutral endopeptidases that can cleave all ECM components and several non-ECM proteins, such as adhesion molecules, cytokines, proteinase inhibitors and other MMPs (Maquoi et al., 2002). MMPs are potential regulators of adipogenesis and adipose tissue growth. For example, MT1-MMP has been demonstrated to be essential for adipogenesis *in vivo* (Chun et al., 2006). In the absence of MT1-MMP, adipose tissue development is disturbed so that only miniature adipocytes are developed and lipodystrophia occurs (Chun et al., 2006). However, the inhibition studies of different MMPs have produced somewhat controversial results and more research is needed to elucidate the functional roles of different MMPs (Mariman & Wang, 2010).

Table 1: The main adipose-derived hormones and adipokines released main growth factors, ECM components and enzymes released by adipose tissue.

Type	Factor	Main cell source	Main function	Main reference
Adipose-derived hormones	Leptin	Adipocytes	Main regulator of the energy balance of the body via hypothalamus, inhibits food intake, increases energy expenditure	(Coelho et al., 2013; Kershaw & Flier, 2004)
	Adiponectin	Adipocytes	Regulates fatty-acid oxidation in liver and muscle, increases insulin sensitivity, signals energy requirement via hypothalamus	(Coelho et al., 2013; Kershaw & Flier, 2004)
	Resistin	Macrophages	Affects insulin action, possible link between obesity and type 2 diabetes	(Galic et al., 2010; Kershaw & Flier, 2004)
Adipokines	Visfatin	Adipocytes	Involved in B-cell maturation, possible role in insulin sensitivity development	(Rasouli & Kern, 2008)
	TNFα	Macrophages	Promotes inflammation, impairs insulin signaling in liver and in adipose tissue	(Galic et al., 2010)
	IL-6	SVF cells	Promotes inflammation, impairs insulin function in peripheral tissues, high expression in type 2 diabetes	(Galic et al., 2010; Kershaw & Flier, 2004)
	IL-1β	SVF cells	Promotes inflammation, Might decrease glucose uptake and Glut-1 receptor translocation in adipocytes	(Jager et al., 2007)
	Chemerin	Adipocytes	Modulator of adipogenesis, regulates metabolic homeostasis in adipocytes	(Goralski et al., 2007)
	PAI-I	SVF cells	Inhibits fibrinolysis, an anticlotting factor, functions in angiogenesis and atherosgenesis	(Kershaw & Flier, 2004; Ronti et al., 2006)
	RBP4	Adipocytes	Impairs insulin signaling in muscle and adipocytes, increases glucose production and enhances gluconeogenesis in liver, causes systemic insulin resistance	(Galic et al., 2010)
Growth factors	VEGF-A	SVF cells, adipocytes	Promotes angiogenesis, key regulator of endothelial cell proliferation and migration	(Christiaens & Lijnen, 2010; G. J. Hausman & Richardson, 2004)
	VEGF-B	SVF cells, adipocytes	Promotes angiogenesis, has a role in ECM degradation	(Christiaens & Lijnen, 2010)
	VEGF-C	SVF cells, adipocytes	Promotes angiogenesis and lymphangiogenesis	(Christiaens & Lijnen, 2010)
	HGF	SVF cells	Promotes and regulates angiogenesis, promotes morphogenic and mitogenic activities in many biological processes	(Bell et al., 2008; Saiki et al., 2006)
	TGFβ	SVF cells	Regulates angiogenesis trough PAI-I regulation, inhibits adipogenesis	(Poulos et al., 2010)
	FGF-1	Adipocytes, preadipocytes	Regulates PPARγ activation	(Jonker et al., 2012)
	FGF-2	Adipocytes, preadipocytes	Promotes differentiation, migration and proliferation of hASCs, promotes angiogenesis	(Poulos et al., 2010)
	Ang-1, Ang-2	Adipocytes, SVF cells	Contributes to blood vessel maintenance, stabilization and growth through TIE-2 receptor activation	(Christiaens & Lijnen, 2010)
ECM components & enzymes	Col-VI	Adipocytes	The main component of ECM basal lamina, involved in adipocyte differentiation, may contribute to the development of obesity-related diseases, may stimulate tumor growth, interacts with other matrix proteins	(Iyengar et al., 2005; Mariman & Wang, 2010)
	MMP-2, MMP-9	SVF cells	Degrade ECM components and remodel ECM, possible regulators of adipocyte differentiation	(Y. Cao, 2010; Mariman & Wang, 2010)
	TIMP-1	SVF cells	Inhibits MMPs, inhibits angiogenesis and adipogenesis, promotes cell growth	(Meissburger et al., 2011; Ries, 2014)

2.5 Vascularization of adipose tissue

Vascularization is essential for the growth, development and repair of all organs and tissues. As adipose tissue is able to either shrink or enlarge depending on the energy balance of the body, also adipose tissue vascular network needs to remodel itself. Enlargement of the adipose tissue can be supported by new blood vessel formation, neovascularization, or by dilating and remodeling of the already existing capillaries (Christiaens & Lijnen, 2010).

2.5.1 Capillaries

Capillaries are the smallest blood vessels of the body. They consist of a single layer of endothelial cells (EC), which are surrounded by the basement membrane and loosely covered by pericytes (Szoke et al., 2012). Capillaries can be either continuous or fenestrated. Fenestrated capillaries have small pores in them and are more permeable than continuous capillaries (Risau, 1998).

EC line the inside of capillaries and larger blood vessels (Kalluri, 2003; Lehle et al., 2010). EC are stable cells, having a turnover time of hundreds of days (Kalluri, 2003). However, during the neovascularization, turnover time of EC can accelerate up to 5 days (Kalluri, 2003). Although vascular EC in general have common features, EC show a high degree of heterogeneity in their gene expression and function, depending on their location (Lehle et al., 2010). Despite the extensive studies, the fundamental molecular mechanisms of EC differentiation are not yet well understood (Lehle et al., 2010).

In adipose tissue, as well as in the most other tissues, the majority of the substance exchange occurs through capillaries. One of the main functions of endothelial cells is to act as a selective barrier between the blood stream and tissues (Goddard & Iruela-Arispe, 2013). Endothelial cells can exchange substances either passively or actively (Vestweber, 2008). The permeability of ECs is controlled by vesicular trafficking, complex junction rearrangements and refined cytoskeletal dynamics (Goddard & Iruela-Arispe, 2013). The highly dynamic and delicate regulation of endothelial permeability thus allows substance exchange to be accelerated or reduced, facilitates immune surveillance and enables the deposition of matrix proteins outside the vascular wall, when repair is needed (Goddard & Iruela-Arispe, 2013). In addition to barrier functions, ECs control haemostasis and vasomotor tone (Lehle et al., 2010).

Basement membranes are about 50 - 100 nm thick specialized extracellular matrices that separate endothelial and epithelial cells from connective tissue and surround fat, muscle and adipose tissue (Morris et al., 2014). The vascular basement membrane consists mostly of collagen IV, laminins, nidogens and perlecan, which is a heparan sulfate proteoglycan (Senger & Davis, 2011). Basement

membrane offers physical support and stabilization to the vessels and together with ECs controls the permeability of capillaries (Senger & Davis, 2011). Basement membrane thickening due to the excess synthesis and/or decreased degradation of its components is one of the most prominent and characteristic features of early diabetic microvessel disease (Roy et al., 1994).

Pericytes are polymorphic, elongated, periendothelial support cells that wrap around the length of microvessels (Sarkar & Schmued, 2012; Stapor et al., 2014). Although capillaries lack the smooth muscle layer present in larger blood vessels, pericytes are able to contract and they express actin and desmin, which are two crusial proteins in smooth muscle function (Sarkar & Schmued, 2012; Stapor et al., 2014). Thus, pericytes may have an important role in blood flow regulation at capillary level (Stapor et al., 2014). It has also been proposed that pericytes would influence on EC action and angiogenesis (Sarkar & Schmued, 2012; Stapor et al., 2014).

2.5.2 Angiogenesis

Neovascularization is typically divided into two different processes. During the embryonic development, the *de novo* -formation of blood vessels occurs through vasculogenesis, where mesoderm-derived angioblasts are organized into blood vessels (Corvera & Gealekman, 2014). In adulthood new blood vessels develop mainly through angiogenesis, where new vessels develop from pre-existing blood vessels (Ucuzian & Greisler, 2007). However, neovascularization is likely to be a more complex process, where vasculogenesis and angiogenesis occur simultaneously in both developmental and adult tissues (Ucuzian & Greisler, 2007). As the majority of the existing *in vitro* models of neovascularization model angiogenesis, only angiogenesis is discussed in detail below. A scheme of angiogenesis and the main events are represented in Figure 2

Angiogenesis is initiated, when a blood vessel senses an angiogenic signal, which is released by a hypoxic, inflammatory or tumour cell (Carmeliet & Jain, 2011). First, pericytes detach from the basal membrane by proteolytic degradation, which is mediated by MMPs (Carmeliet & Jain, 2011). MMPs degrade also ECM in co-operation with the suppressors of protease inhibitors (Jain, 2003). Nitric oxide dilates the existing vessels and VEGF increases the permeability of the endothelial cell layer that leads to the leaking of plasma proteins from the nascent vessels (Jain, 2003). These plasma proteins serve as a temporal migration matrix for endothelial cells as they move with the help of integrin interactions (Carmeliet & Jain, 2011). Endothelial cells also start to proliferate in response to VEGF and other mitogenic signals (Jain, 2003). One endothelial cell becomes a tip cell, which leads the tip in the presence of factors such as VEGF receptors, neuropilins and Notch

ligands DLL4 and JAGGED1 (Carmeliet & Jain, 2011).

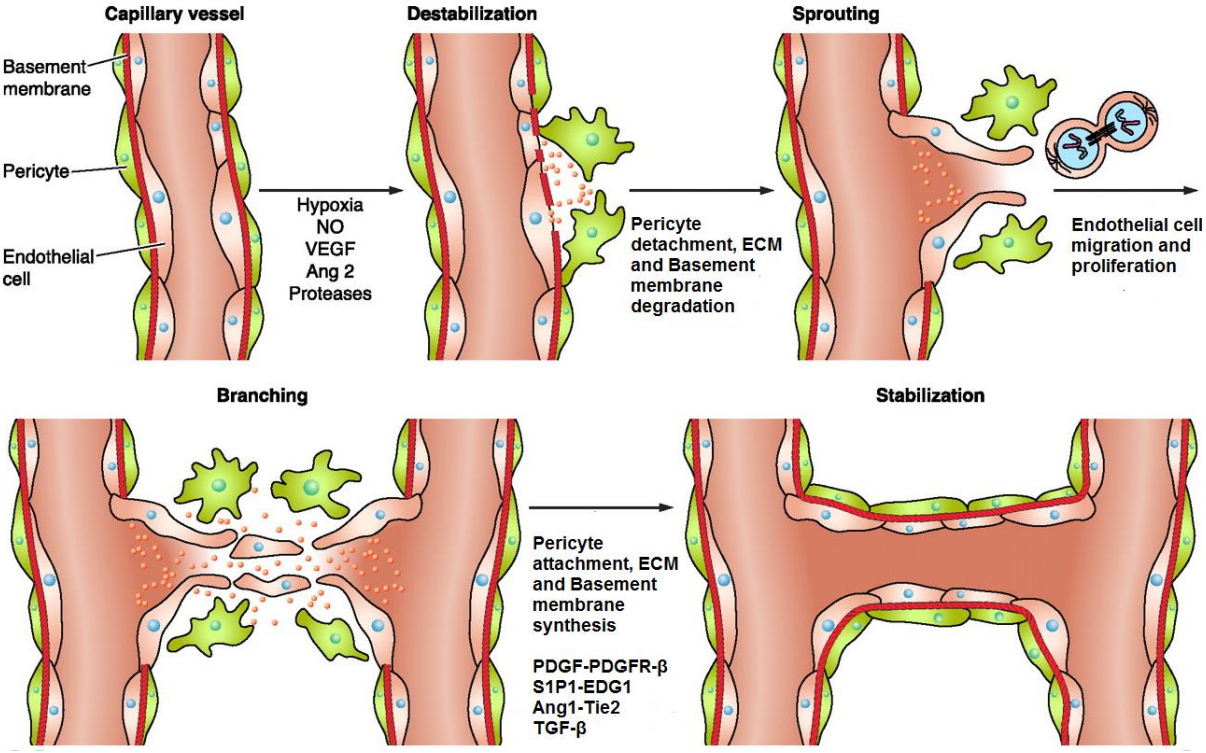

Figure 2 : The main events and regulators of angiogenesis. Angiogenesis initiates, when a hypoxic, inflammatory or tumor cell releases angiogenic signal (such as VEGFs or Ang2) that a vessel senses. Pericytes then detach from the vessel wall and basement membrane and ECM are degraded by proteases and the degradation is controlled by the protease inhibitors (MMPs and e.g.TIMP-2). Endothelial cells migrate and proliferate, tip cell as their leader. Ephrin, neuropilins and cues from basement membrane and ECM regulate branching of vascular networks. Finally vessels are stabilized by pericyte attachment and ECM and basement membrane re-building. Modified from (Clapp et al., 2009).

The immature vessels are stabilized by recruiting mural cells, either pericytes or smooth muscle cells, and by forming ECM (Gerhardt & Betsholtz, 2003). Four pathways have been recognized to be involved in the stabilization process: (1) PDGF and B-PDGF receptor (PDGFR-β), (2) sphingosine-1-phosphate-1 (S1P1) and endothelial differentiation sphingolipid G-protein coupled receptor 1 (EDG1), (3) Ang1-Tie-2 and (4) transforming growth factor β (TGF-β) (Jain, 2003). PDGF-PDGFR-β and S1P1-EDG1 pathway function both in recruiting mural cells (Carmeliet & Jain, 2011; Jain, 2003) whereas Ang1-Tie-2 pathway is needed to further stabilize the endothelial cell–mural cell interactions (Jain, 2003) and TGF-β to induce genes, which products are necessary for basement membrane formation (Holderfield & Hughes, 2008).

The final maturation of vascular networks involves the optimal patterning of the network. The same signalling pathways that control the evolvement of the nervous system, such as ephrins and neuropilins, also coordinate the development of vascular networks (Jain, 2003). In addition,

basement membrane and ECM produce cues for network development by regulating the proliferation, migration, survival and differentiation of endothelial and mural cells (Jain, 2003).

2.5.3 Angiogenic triggers in adipose tissue

Two different possibilities for angiogenic growth triggers in adipose tissue have been proposed. In the first option, angiogenesis in adipose tissue is a response to hypoxia, which is caused by the enlargement of adipocytes and/or proliferation of adipocytes (Corvera & Gealekman, 2014). In the second option, angiogenesis in adipose tissue is a result of developmental and/or metabolic signals (Corvera & Gealekman, 2014). Thus, blood vessels would develop before adipocyte growth and/or proliferation or parallel to it (Corvera & Gealekman, 2014).

There are several studies that support the first option. In mice studies, adipose tissue has shown to become hypoxic in response to obesity that has been accomplished with high-fat diet (Corvera & Gealekman, 2014). Human adipose tissue has also been found to be hypoxic in a study done with microelectrodes (Pasarica et al., 2009). The reported levels of hypoxia were however relatively small and they did not activate classic hypoxia targets, such as VEGFs (Pasarica et al., 2009). In addition, it has been discovered that adipose tissue enlargement in response to high-fat diet in mice does not increase blood flow correspondingly (Trayhurn, 2013).

However, there are *in vitro* studies to support the hypoxia theory. It has been noticed that the expression and secretion of proangiogenic factors is stimulated, when the culturing conditions are low of oxygen (Lolmede et al., 2003). The evidence for hypoxia theory remains thus inconclusive, so it might not be alone sufficient to trigger angiogenesis in adipose tissue.

The evidence to support the second option relies on developmental studies. During fetal development, angiogenesis/vasculogenesis precedes adipogenesis and blood vessel ECM develops before adipose tissue ECM development (G. J. Hausman & Richardson, 2004). VEGF expression and the following angiogenesis may increase or precipitate adipogenesis also in postnatal development (G. J. Hausman & Richardson, 2004). In addition, antiangiogenic treatments for mice have shown to decrease fat pad weights 12 - 22 % and decrease body weights in a dose-dependent and reversible manner (Rupnick et al., 2002).

2.6 Adult stem cells

Stem cells are typically categorized into embryonic stem cells, induced pluripotent stem cells (iPS cells) and adult stem cells. Embryonic stem cells and iPS cells have almost unlimited differentiation potential *in vitro* and *in vivo*, but the use of these cells is limited by ethical, legal and political concerns as well as by clinical and scientific issues of safety and efficacy (Lindroos et al., 2011).

Thus, although adult stem cells have lower differentiation capacity, they offer a less controversial alternative to embryonic stem cells and are considerably cheaper to produce than iPS cells (Lindroos et al., 2011).

Adult stem cells (also called mesenchymal stem cells and somatic stem cells) are undifferentiated cells that are found in a specific tissue or organ (Gomillion & Burg, 2006). Adult stem cells have been found in e.g. from bone marrow, blood, adipose tissue, synovium, deciduous teeth, liver and spleen (Baer, 2014). In general, adult stem cells are self-renewing and multipotent cells that are easily isolated, cultured and expanded in laboratory settings (Gomillion & Burg, 2006).

Adult stem cells are typically obtained either from bone-marrow (BMSCs, bone-marrow-derived stem cells) or from adipose tissue (ASCs, adipose-derived stromal cells). BMSCs have excellent proliferating capacity and they can differentiate to wide variety of cell types (Cai et al., 2011; Lindroos et al., 2011). However, the harvesting of BMSCs by bone marrow aspiration is painful for the donor and the number of cells obtained is usually low (Cai et al., 2011; Lindroos et al., 2011). Thus, adipose tissue is an attractive choice of cell source, as ASCs are relatively easy to harvest by liposuction or lipoplasty, have lower donor-site morbidity and are available in greater number (Kokai et al., 2014).

2.6.1 Adipose stromal cells

Like BMSCs, also ASC have potential to differentiate into multiple lineages. ASC have been shown to be able to differentiate into cells of ectodermal, mesodermal and endodermal origin (Tsuji et al., 2014). These cells include adipocytes, myocytes, osteoblasts, chondrocytes, neurons, endothelial cells and hepatocytes (Kokai et al., 2014). In addition, ASC are genetically more stable in a long-term culture when compared with BMSCs (Lindroos et al., 2011). ASC have also been demonstrated to have immunosuppressive properties (Lindroos et al., 2011). ASC inhibit the proliferation of activated lymphocytes *in vitro* and have been noticed to alleviate graft-versus-host diseases in mice (Kokai et al., 2014). ASC also secrete several soluble factors, such as angiogenic factors (e.g. VEGF), anti-apoptosis factors (e.g. IGF-1), hematopoietic factors (e.g. colony stimulating factors and interleukins) and hepatocyte growth factor (Ong & Sugii, 2013). Thus, ASC are promising cell candidates to several regenerative clinical applications.

ASC have been used by now in soft tissue, skeletal tissue, heart, immune disorder, neurodegeneration and gene therapy applications (Gimble et al., 2012; Lindroos et al., 2011). Several clinical studies with ASCs have been made and have shown promising results, but yet more

studies are needed to verify the clinical safety and reproducible utilization of these cells (Lindroos et al., 2011).

2.7 Adipogenesis assays

2.7.1 *In vitro* assays

Much of what is known about the molecular mechanisms of adipogenesis is based on studies done with adipogenic cell lines. Currently available cell models include preadipocyte cell lines that are already committed to the adipocyte lineage and multipotent stem cells that are able to commit to different lineages, including adipocyte, muscle and bone lineages (Armani et al., 2010). Multipotent stem cells used in adipogenesis assays include embryonic stem cells and SVF cells obtained from adipose tissue.

3T3-F442A and 3T3-L1 cell lines are considered the most frequently used preadipocyte lines (Armani et al., 2010; Gregoire et al., 1998). They are both originally clonally isolated from the Swiss 3T3 cell line, which is derived from disaggregated 17- to 19-day-old mouse embryos (Green & Meuth, 1974; Green & Kehinde, 1976). Clonal cell lines are homogenous in terms of cellular population and they exhibit the same phase of differentiation, which allows homogenous response to different treatments (Armani et al., 2010). In addition, these cells can be passaged indefinitely (Ntambi & Young-Cheul, 2000). Other common preadipocyte cell lines include Ob17 cell line, which is generated from the fat pads of genetically obese (*ob/ob*) adult mouse, and TAI cell line, which is established by treating CH310T1/2 mouse embryo fibroblast cells with the demethylating agent 5-azacytidine (Gregoire et al., 1998).

Although preadipocyte cell lines share similarities with primary adipocytes and are useful when studying adipogenesis, they have some important properties that differ from primary adipocytes. For example, leptin is expressed at much lower concentrations than in primary adipocytes (Cristancho & Lazar, 2011). Thus, SVF-derived cultures may reflect the real *in vivo* context better than preadipocyte cell lines (Armani et al., 2010). Another advantage of SVF-derived cultures is that cells can be obtained from various species (including humans) and from different fat depots, which enables the study of differences between species and depots (Gregoire et al., 1998). However, the heterogeneity of SVF-derived cell cultures may be a problem as well as the fact that the cultures have a limited life span, which restrains their time window for experimental procedures (Gregoire et al., 1998; Scroyen et al., 2013).

Pluripotent embryonic stem (ES) cells have also been studied as a model system for adipogenesis. These cells have been derived from the inner mass of 3,5-day-old mouse blastocyst (Armani et al.,

2010). Differentiating ES cells into committed preadipocytes require retinoic acid treatment of ES cell-derived embryonic bodies before induction with standard adipogenic hormones (Armani et al., 2010).

In order to achieve maximal adipogenic differentiation, cell culture models are treated with adipogenic cocktails. The nature of the induction is dependent of the specific cell culture model used, as the responsiveness of cells obtained from different sources varies (Gregoire et al., 1998). However, the standard adipogenic cocktail includes typically supraphysiological concentrations of insulin, dexamethasone (DEX) and isobuthylmethylxanthine (IBMX) (Gregoire, 2001). DEX is a synthetic glucocorticoid agonist, which stimulates adipogenesis by the glucocorticoid receptor pathway, whereas IBMX is a cAMP phosphatase inhibitor that stimulates the cAMP-dependent kinase pathway (Armani et al., 2010; Ntambi & Young-Cheul, 2000). Also other adipogenic factors, such as indomethacin, glucocorticoids, troglitazone and triiodothyronine, are commonly used in adipogenic cocktails (Armani et al., 2010).

2.7.1.1 Adipose tissue extract for in vitro adipogenesis induction

Also new ways apart from chemical induction to elicit adipogenesis have been studied. Sarkanen *et al.* developed adipose tissue extract (ATE, patent number WO2010026299A1), which has been proven to induce adipogenesis and angiogenesis *in vitro* (Sarkanen et al., 2012a). ATE is a cell-free product, which is extracted from mature human adipose tissue without affecting cell viability (Sarkanen et al., 2012a).

Adipogenic differentiation of human adipose stromal cell (hASC) cell cultures treated with ATE was shown in less than one week, when ATE concentration was at least 200 µg/ml, measured in total protein content (Sarkanen et al., 2012a). ATE treatment results in the homogenous differentiation of hASC cells into mature adipocytes and induces an accelerated and up to fourfold higher triglyceride accumulation, when compared with control adipogenic cocktail treatment, which included adipogenesis inducing agents DEX, insulin, indomethacin and IBMX (Sarkanen et al., 2012a; Verseijden et al., 2009).

2.7.2 *In vivo* assays

Although some events of adipogenesis can be studied directly with humans, the possible toxicity of most of the experimental methods limits the use of human studies (Spalding et al., 2008). Thus, mouse remains the most used *in vivo* model for adipogenesis and adipose tissue biology (Bluher, 2005; Q. A. Wang et al., 2014).

Methods in order to study expansion of adipocyte size (hypertrophy) and number (hyperplasia) *in vivo* have relied traditionally on quantification of cell size and number (Jo et al., 2009) and BrdU or radiolabeling "pulse-chase" experiments to quantify the incorporation of the label into mature adipocytes (Joe et al., 2009; Lee et al., 2012). There are some key assumptions that have to be done when using these methods. In cell size and number quantification method, cell size is a surrogate for the age of the cell, where small cells represent new adipocytes and large cells adipocytes undergoing hypertrophy (Jo et al., 2009). However, differences in the sizes of adipocytes might only be a result from different lipid handling. Quantification of adipocyte number can also be challenging from a technical point of view, as adipose tissue is heterogeneous tissue (Q. A. Wang et al., 2014). In the BrdU method, progenitor cells are thought to proliferate before differentiation into adipocytes (Lee et al., 2012). Although this is a reasonable assumption, recent findings suggest that this might not always be the case (Q. A. Wang et al., 2014).

In order to study adipose tissue biology, several transgenic and knock-out mouse models have been developed. The promoters for adipocyte lipid binding protein 2 (AP2) and for phosphoenolpyruvate carboxykinase are commonly used to target both white and brown adipose tissue, when studying adipose tissue-specific gene expression or knock-out (Bluher, 2005). Transgenic mouse models have been recently developed to model also adipogenesis. For example, "AdipoChaser" mice have been created by combining three published transgenic lines. They can be used when tracing adipogenesis that occurs during high-fat feeding or in response to cold exposure (Q. A. Wang et al., 2014).

2.7.2.1 In vivo models for adipose tissue related diseases

A large number of *in vivo* models, especially mouse models, have been generated in order to study adipose tissue related diseases, such as obesity and type 2 diabetes (Chandrasekera & Pippin, 2014; Lai et al., 2014). These disease models have also been used to produce basic knowledge of adipogenesis. Available mouse obesity and type 2 diabetes models can be divided into two main groups: nutritionally induced obesity and/or type 2 diabetes and genetically induced obesity/type 2 diabetes (Lai et al., 2014; Scroyen et al., 2013). Diet induced obesity models are sometimes also combined with chemical, surgical or genetic type 2 diabetes induction (Lai et al., 2014).

Nutritionally induced obesity is usually achieved with high-fat diet (HFD) feeding. Although the term HFD is widely used, there is no standardized HFD, where the exact fat content or composition would have been defined (Buettner et al., 2007). Fat content of HFD varies typically between 20 - 60 % and the basic fat component varies between animal-derived fats to vegetable oils (Buettner et

al., 2007). Also high-carbohydrate diets, such as high-fructose and high-sucrose diets have been used alone or in combination with HFD in order to elicit the events of the metabolic syndrome (Lai et al., 2014). Problem with the nutritionally induced obesity mouse models is that different mouse strains response to diet varies greatly (Scroyen et al., 2013). In addition, the experimental circumstances of the test animals affect their eating habits. It is thus difficult to compare results obtained by different laboratories with each other and human translatability is also limited (Lai et al., 2014).

Genetically induced obesity is typically studied with mice deficient in leptin (*ob/ob*) or leptin receptor (*db/db*) (Lijnen, 2011). Genetically induced type 2 diabetes in mice is usually achieved with the gene manipulation of the insulin receptor, insulin receptor substrate subtypes, protein-kinase B or glucose-transporter 4 (LeRoith & Gavrilova, 2006). Manipulation of these genes can be targeted to various tissues, e.g. adipose tissue, muscle, liver and the β-cells in pancreas, in order to mimic the insulin resistance seen in pre-diabetes and type 2 diabetes (LeRoith & Gavrilova, 2006).

2.8 Adipose tissue *in vitro* models for tissue-engineering applications

In vitro models of adipose tissue are an interesting area of research also from the tissue-engineering point of view. Current repair methods for soft tissue reconstruction include autologous transplants and commercially available fillers. These approaches have however some serious disadvantages, such as volume loss and site morbidity, that could be overcome with tissue-engineered adipose tissue (Gomillion & Burg, 2006).

2.8.1 Key requirements and analysis methods for tissue-engineered adipose tissue

Key requirements for tissue-engineered adipose tissue include host compatibility, bioactivity and sustainability (J. H. Choi et al., 2010). Host compatibility is an essential remark for any tissue-engineered construct, so that the construct does not elicit immunorejection in the body (Levenberg & Langer, 2004). For soft tissue reconstruction, also site specificity might play an important role. Several studies have shown that soft tissue site has an effect both on the degree of adipose tissue regeneration and the metabolic function of regenerated tissue (J. H. Choi et al., 2010). Considering the detected differences between different fat depots in the body (Hyvonen & Spalding, 2014), the results are not surprising, but need to be taken into account, when designing engineered adipose tissue.

In addition to host compatibility, the mechanical properties and the degradation profile of the implanted scaffold biomaterial are critical when creating desired conditions for tissue formation (Lavik & Langer, 2004). It is also important that the bioactivity of the regenerated adipose tissue

mimics the bioactivity of native adipose tissue. This means that the regenerated tissue has the same function and structure as the native tissue. Thus, regenerated adipose tissue should contain functional vasculature, nerves and lymph supply (D. B. Hausman et al., 2001).

Several assays to elucidate the properties of tissue-engineered adipose tissue have been created. Typically measured variables are lipid droplet formation, adipocyte gene expression, adipose tissue secretory product expression, metabolic activity and vasculature incorporation (J. H. Choi et al., 2010). Common methods to evaluate these variables are listed in Table 2.

2.8.2 Current human vascularized adipose tissue models

Current human vascularized adipose tissue models are typically constructed by co-culturing human adipose stromal cells (hASC) or preadipocytes with endothelial cells (Kang et al., 2009). Kang *et al.* have developed vascularized adipose tissue *in vitro* by culturing hASCs and human umbilical cord vein endothelial cells (HUVECs) on a porous silk protein scaffold (Kang et al., 2009). Also Borges *et al.* have been developing vascularized adipose tissue *in vitro* by culturing human preadipocytes with human endothelial cells in a fibrin glue matrix on a chick chorioallantoic membraine (Borges et al., 2003; Borges et al., 2007). Wittmann *et al*. used also fibrin gels as scaffolds in their hASC based *in vivo* vascularized adipose tissue model (Wittmann et al., 2015).

Table 2: Common methods to evaluate tissue-engineered adipose tissue. Modified from (J. H. Choi et al., 2010).

Measured variable	Method
Adipocyte morphology	Oil-red-oil Adipored Triglyceride quantification assays
Adipocyte gene and enzyme expression	RT-qPCR
Adipose tissue secretory product expression	ELISA
Metabolic activity	Lipolysis assay Glucose uptake
Vasculature incorporation	Histology Immunohistochemistry

3. Aim of the Study

The main goal of this study was to develop a vascularized adipose tissue model by combining adipogenesis and angiogenesis cell models, and optimize and characterize it, so that it can be validated and finally used as a tool in adipose tissue research and in the *in vitro* testing of chemicals and drugs. The specific aim of this study was to find out how the vascularized adipose tissue model, constructed of hASC-HUVEC co-culture, would be the most optimally created to resolve the issues in maturity and detachment. The examined questions regarding the optimal construction of the vascularized adipose tissue model were to:

1) Determine whether adding tubules to adipose tissue model results in improvement of the maturity of the adipocytes
2) Determine whether proper vascular structures are formed when cultured with adipocytes
3) Determine if the problem of too early cell detachment can be solved by changing the plating and differentiation scheme

4. Materials & Methods

4.1 Cell culture

4.1.1 Cell culturing of human adipose stromal cells

The human adipose stromal cells (hASC) used in the study were heterogenous cell populations obtained by isolating the stromal vascular fraction cells of human adipose tissue. Adipose tissues were obtained from plastic surgeries conducted at Tampere University Hospital. The isolation and use of hASC have been approved by the Ethics committee of the Pirkanmaa Hospital district. hASC were isolated by mechanically cutting and digesting the adipose tissue with collagenase type I (Sarkanen et al., 2012b). The isolated hASC were expanded in hASC medium and cryopreserved in vapor phase nitrogen at passage 0. Before cryopreservation, mycoplasma contamination was tested with Mycoplasma kit (MycoAlert® Detection Kit, Lonza Group LTD, Basel Switzerland).

Primary hASC were thawed in 37ºC water bath (OLS200, Grant instruments, Cambridge, UK) the maximum of 2 minutes and then transferred into a 15 ml polypropylene tube (Sarsted, Nürnberg, Germany) containing 10 ml preheated hASC medium (Table 3). After this, hASC were centrifuged (Biofuge PrimoR, Heraeus, Hanau, Germany) at 131 x g at room temperature (RT) for 5 minutes. Then, supernatant was removed and cells were resuspended to 1 ml of preheated hASC medium. Resuspended cells were then transferred into a 75 cm^2 cell culture flask, which contained 9 ml preheated hASC medium. The cell culture flask was swirled so that the cells would spread evenly in the culture flask.

Cells were cultured in a humidified carbon dioxide (CO_2) incubator MCO-17AI (Sanyo Electrics Co., Ltd., Osaka, Japan) at 37ºC in 5% CO_2 atmosphere. The proliferation and morphology of hASC were monitored with Olympus CK 40-F200 microscope (Olympus Corporation, Tokyo, Japan). The culture media was changed every second or third day. hASC were cultured for 7 - 9 days in the cell culture flasks before using them in experiments.

4.1.2 The cell culturing of human umbilical cord vein endothelial cells

Human umbilical cord vein endothelial cells (HUVEC) used in the study were isolated from donated umbilical cords. The donated umbilical cords were obtained from scheduled Cesarean sections conducted at Tampere University Hospital. The isolation and use of HUVEC have been approved by the Ethics committee of the Pirkanmaa Hospital district. HUVEC were isolated by the cannulation of the umbilical vein and infusing the vein with collagenase I (Sarkanen et al., 2012b). The isolated HUVEC were expanded in HUVEC medium and cryopreserved in vapor phase

nitrogen at passage 2. Mycoplasma contamination was tested before cryopreservation with Mycoplasma kit (Lonza Group LTD).

HUVEC were thawed in 37ºC water bath (OLS200, Grant instruments) the maximum of 2 minutes and then transferred into a 15 ml polypropylene tube (Sarsted) containing 10 ml preheated HUVEC medium (Table 3). HUVEC were then centrifuged (Biofuge PrimoR, Heraeus) at 131 x g at RT for 5 minutes. After this, supernatant was removed and cells were resuspended to 1 ml of preheated HUVEC medium. Then, resuspended HUVEC were pipetted into 75 cm^2 cell culture flask, which contained 9 ml pre-heated HUVEC medium. The cell culture flask was swirled in order to get the cells spread evenly in the culture flask.

HUVEC were cultured in the incubator (Sanyo) at 37ºC in 5% CO_2 atmosphere. The proliferation and morphology of HUVEC were monitored with Olympus CK 40-F200 microscope. HUVEC were cultured 3 days in cell culture flasks before their use in experiments.

Table 3: List of cell culture media and their components.

Medium	Components	Manufacturer
hASC medium	Dulbecco's modified Eagle's medium Nutrient Mixture F-12 (DMEM/F-12) 10 % human serum 2 mM L-Glutamine	Gibco (Life technologies, Carlsbad, USA) Lonza Group LTD Gibco
HUVEC medium	EBM-2 Single-Quots supplements: IGF-1, VEGF, FGF-β, Fetal Bovine Serum, Hydrocortisone, Heparin, Ascorbic Acid, Epidermal growth factor	Lonza Group LTD Lonza Group LTD

4.1.3 Building the hASC-HUVEC co-culture

hASC were first rinsed with 1 ml of preheated Tryple™ express (Gibco), which was immediately removed. Then, 2.5 ml of Tryple™ express was added into the cell culture flask to detach the cells from the bottom of the flask. Tryple™ express containing flasks were incubated in the incubator for 6 - 10 minutes and after the cells had detached, they were suspended into 5 ml of preheated HUVEC medium, transferred to a 15 ml polypropylene tube (Sarsted) and centrifuged (Biofuge PrimoR, Heraeus) at 131 x g at RT for 5 minutes. After that, supernatant was removed carefully and the cell pellet was resuspended into 0.5 ml of HUVEC medium.

An aliquot of cell suspension was stained and diluted 1:10 with Trypan Blue (Sigma Aldrich, St. Louis, MO, USA) and the cells were counted with Bürker's chamber (Assistent®, Glaswarenfabrik, Karl Hecht KG, Rhön, Germany). Cells were then diluted to an appropriate volume of HUVEC medium and plated in a density of 22 000 cells/cm^2 on 48-well Nunclon™ Δ-Surface (Sigma Aldrich) plates. hASC were at passage 2 in the model.

If HUVEC were added on top of hASC on the same day hASC were seeded, hASC were allowed to attach to the well bottoms for 1 hour before adding HUVEC. HUVEC were detached from the cell culture flasks and counted like hASC and plated in a density of 4400 cells/cm^2. HUVEC were at passage 4 in the model. Altogether, 3 different hASC-HUVEC combinations were used. All strategies were tested with all the hASC-HUVEC combinations, so that possible batch to batch variations could be eliminated. The used hASC-HUVEC combinations in different experiments are listed in Appendix 1.

4.2 hASC-HUVEC co-culture differentiation into vascularized adipose tissue

The differentiation was begun on day 1 by exposing hASC-HUVEC co-cultures to adipogenic and angiogenic differentiation media, as shown in Figure 3, in order to achieve vascularized adipose tissue. Adipose tissue extract, ATE was used as a base solution for adipogenic differentiation medium, ATE medium. ATE was prepared by cutting adipose tissue specimens into small pieces and then incubating the pieces with DMEM/F12 and finally sterile-filtering the extract (Sarkanen et al., 2012a). In this study, ATE was used at total protein concentration of 1800 µg/ml. The list of ATE-medium components is represented in Table 4. Altogether, 6 different ATE batches were used. In order to eliminate possible batch to batch variation on the results, all strategies were treated with all the different ATE batches. ATE batches used in this study are listed in Appendix 2.

The content of angiogenic differentiation medium, angiogenesis stimulation medium, has been optimized before (Huttala et al., 2015). Angiogenesis stimulation medium was supplemented with serum free medium. The contents of both stimulation medium and serum free medium are listed in Table 4.

Cultures were exposed to one differentiation medium at a time so that 500 µl of differentiation medium was pipetted on the cell cultures and changed on each 2 - 3 day. Each cell culture was exposed twice (exposures 1 and 2) to either adipogenic or angiogenic medium and then twice (exposures 3 and 4) to the remaining differentiation medium. Thus, each cell culture was exposed in total four times during the 14 day long cell culturing. The study design for differentiation is

represented in Figure 3. Different differentiation order strategies were tested and they are discussed in detail in the following section.

Table 4: List of differentiation media components.

Medium	Components	Manufacturer
ATE medium	DMEM/F-12	Gibco
	Adipose tissue extract (different batches)	Own production
	ATE-supplement:	Lonza Group LTD
	10 % Human Serum	PAA Laboratories (Pasching, Austria)
	2 mM L-Glutamine	Gibco
	Penicillin-Streptomycin:	Gibco
	50 units/µl Penicillin	
	50 µg/µl Streptomycin	
Serum free medium	DMEM/F-12	Gibco
	1 % Bovine Serum Albumin (BSA)	Biosera (Boussens, France)
	2,8 mM Sodium Puryvate	Gibco
	2,56 mM L-Glutamine	Gibco
	ITS-supplement:	BD Biosciences (Franklin Lakes, USA)
	6,65 µg/ml Insulin	
	6,65 µg/ml Transferrin	
	6,65 ng/ml Selenious	
	0,1 nM 3,3,5-Triiodo-L-thyronine sodium salt	Sigma Aldrich
Angiogenesis stimulation medium	Serum free medium	
	200 µg/ml Ascorbic Acid:	
	Ascorbic Acid	Sigma Aldrich
	0,1 M NaOH	Fluka (Sigma-Aldrich, St. Louis, MO, USA)
	2 µg/ml Hydrocortisone:	
	Hydrocortisone	Sigma Aldrich
	abs. EtOH	Altia (Helsinki, Finland)
	1 ng/ml FGF-β	R&D Systems (Abingdon, UK)
	10 ng/ml VEGF	R&D Systems
	0,5 µg/ml Heparin:	
	Heparin	Sigma-Aldrich
	Sterile Water	Gibco

4.3 hASC-HUVEC co-culture plating & differentiation strategies

In order to find out the optimal plating time for hASC and HUVEC with respect to the differentiation of the cells into adipocytes and blood vessels, six different strategies were tested. Also different amounts of hASC were tested. The details about the plating times and differentiation schemes of different strategies are represented in Table 5.

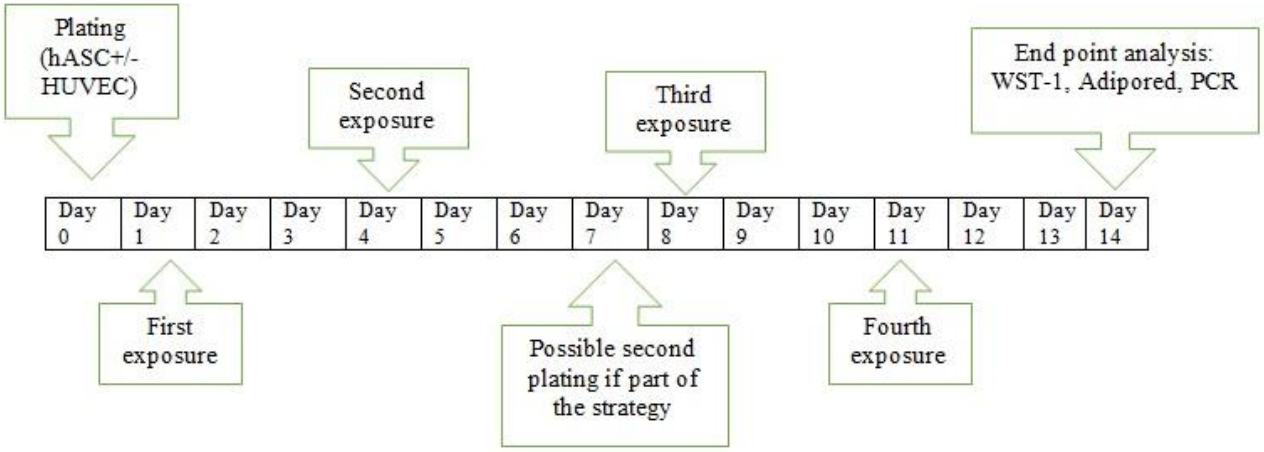

Figure 3: Study design for hASC-HUVEC co-culture plating and differentiation.

Table 5: Plating and differentiation details of different strategies tested for hASC-HUVEC co-culturing.

Strategy	hASC plating day	Number of hASCs plated/well	HUVEC plating day	Number of HUVECs plated/well	Differentiation order
1	Day 1 Day 8	22 000 cells 22 000 cells	Day 8	4400 cells	1.ATE medium 2.Angiogenesis stimulation medium
2	Day 1	44 000 cells	Day 1	4400 cells	1.ATE medium 2.Angiogenesis stimulation medium
3	Day 1	44 000 cells	Day 1	4400 cells	1 Angiogenesis stimulation medium 2. ATE medium
4	Day 1 Day 8	22 000 cells 22 000 cells	Day 1	4400 cells	1 Angiogenesis stimulation medium 2. ATE medium
5	Day 1	22 000 cells	Day 1	4400 cells	1.ATE medium 2.Angiogenesis stimulation medium
6	Day 1	22 000 cells	Day 1	4400 cells	1 Angiogenesis stimulation medium 2. ATE medium

4.3.1 Control samples

Positive controls and negative controls were used to verify the reliability of the results. Both blood vessels (tubules) and fat had their own positive controls. Two negative controls were used, with varying hASC number, corresponding to the number of hASC plated in the wells in different strategies, other having 22 000 and other 44 000 hASC per well. The control cultures were cultured on the same 48-well plates as the actual samples. Tubule (blood vessel) control was exposed only to angiogenesis stimulation medium, fat control only to ATE medium and negative controls to serum free medium. The details of control samples are listed in Table 6.

Table 6: Plating details of control samples.

Control	hASC plating day	Number of hASC plated/well	HUVEC plating day	Number of HUVEC plated/well	Differentiation medium used
Negative 1	Day 1	22 000 cells	Day 1	4400 cells	Serum free medium
Negative 2	Day 1	44 000 cells	Day 1	4400 cells	Serum free medium
Blood vessel	Day 1	22 000 cells	Day 1	4400 cells	Angiogenesis stimulation medium
Fat	Day 1	22 000 cells	-	-	ATE medium

4.4 Cell culture measurements

4.4.1 Triglyceride accumulation measurement

Triglyceride accumulation to the cell cultures was measured with Adipored assay reagent (Lonza Group LTD) and with Varioskan flash multimode reader (Thermo Fischer Scientific, Waltham, MA, USA). Adipored assay was performed on the 14th day of cell culturing (Figure 3), by first removing differentiation media from the wells, then carefully rinsing each well with 400 µl of phosphate buffered saline (PBS) (Lonza Group LTD) and after removal the rinsing-PBS, adding 412 µl of a mixture of Adipored (Lonza Group LTD) assay reagent (12µl) and PBS (400µl) to each well. Then, the plates were incubated in the incubator (Sanyo) at 37ºC for 10 minutes. Finally, the fluorescence was measured with Varioskan flash multimode reader (Thermo Fischer), with excitation at 485 nm and emission at 572 nm. Absorbance values were given as a mean of multipoint calculation.

4.4.2 The relative cell number definition

The relative cell number was spectrophotometrically defined with Cell proliferation reagent WST-1 (Roche Diagnostics, Basel, Switzerland) and with Varioskan flash multimode reader (Thermo Fischer Scientific). WST-1 assay was performed on the 14th day of cell culture (Figure 3) by adding 50µl of WST-1 reagent (Roche Diagnostics) to each well, incubating the plates in CO_2 incubator MCO-17AI (Sanyo) at 37ºC for 60 minutes and then shaking the plates for 1 minute in the dark on a shaker. Finally, the absorbance was measured at 450 nm. Absorbance values were given as a mean of multipoint calculation.

4.4.3 Quantification of triglyceride accumulation

In order to quantify the amount of accumulated triglycerides per cell, Adipored assay absorbance values were divided with WST-1 assay absorbance values. Before that, absorbance values were first normalized to the average of the absorbance values of negative samples of each run. Normalization

and Adipored/WST-1 ratio calculations were made with Microsoft Excel 2010 (Microsoft Corporation, Redmond, Washington, USA). Results were plotted in GraphPad Prism (GraphPad Software Inc., La Jolla, California, USA), where columns represent the mean values and error bars standard deviations.

4.5 Immunocytochemical stainings

To visualize and analyze tubule formation, immunocytochemical stainings were performed. Stainings were made as double-stainings, where both endothelial cells and basement membranes of blood vessels were stained. Stainings were made to the same cell cultures, which were used for Adipored and WST-1 measurements.

Before immunocytochemical stainings, cells were fixed. At first, cells were washed two times with Dulbecco's phosphate buffered saline (DPBS) and then fixed with 4 % paraformalaldehyde at RT for 20 minutes. Then, cells were washed again two times with DPBS. After fixation, cells were permeabilized with 0.5 % Triton-X100 (MP Biochemicals, Santa Ana, CA, USA) at RT for 15 minutes. Cells were then washed two times with DPBS. Next, cells were incubated with 10 % BSA (Roche Diagnostics) at RT for 30 minutes to block unspecific binding sites. After this, primary antibodies diluted in 1 % BSA in DPBS was added on the cells and incubated for 1h at RT or overnight at +4ºC. Two different primary antibodies were used: (1) Anti-von Willebrant factor IgG (anti-vWf IgG, produced in rabbit, Sigma Aldrich), diluted in ratio 1:100, to target endothelial cells and (2) Anti-Collagen IV IgG (anti-ColIV IgG, produced in mouse, Sigma Aldrich), diluted in ratio 1:500, to target the basement membranes of blood vessels.

After primary antibody treatment, cells were washed with DPBS two times and then incubated for 40 minutes with secondary antibodies diluted in 1% BSA in DPBS at RT. FITC-labeled goat polyclonal antibody anti-mouse IgG (Sigma Aldrich), diluted in ratio 1:100, was used to visualize collagen IV and TRITC-labeled goat polyclonal antibody anti-rabbit IgG (Sigma Aldrich), diluted in ratio 1:50, to visualize von Willebrant factor. Cells were then washed two times with DPBS. Finally, DPBS was added and left to the wells and plates were sealed with parafilm. Plates were protected from light and stored at +4ºC until microscopic or Cell-IQ analysis.

4.6 Microscopic analyses

4.6.1 Fluorescence microscopy

After immunocytochemical stainings, tubule structures and triglyceride accumulation were investigated and imaged with Nikon Eclipse Ti-S inverted fluorescence microscope (Nikon, Tokyo,

Japan) and Nikon digital sight DS - U2 camera (Nikon). Images were processed with NIS Elements (Nikon) and Adobe Photoshop CS3 software (Adobe Systems Incorporated, San Jose, CA, USA).

4.6.2 Confocal microscopy

The three-dimensional imaging of tubular networks was performed with a confocal microscope. Microscopic imaging was done with LSM710 and with Zeiss Axio Observer Z1 inverted microscope (Carl Zeiss, Oberkochen, Germany). In order to investigate the 3D-structures and thicknesses of tubular networks, z-stack images were obtained. Z-stack images were taken to cover the whole thickness of the vascular structures, so that in total 25 images were taken. Images were further processed with ZEN 2012 software (Carl Zeiss) and Adobe Photoshop CS3 software (Adobe Systems Incorporated).

4.6.3 Cell-IQ image analysis

In order to investigate the area of tubular networks, cell cultures were imaged with Cell-IQ (CM Technologies Oy, Tampere, Finland). Wells of cell culture plates were imaged with 10x objective and with a grid of 5x5 so that large area of the well was imaged. Grids of each well were then stitched together with Cell-IQ Analyzer (CM Technologies Oy).

Cell-IQ images were further analyzed with ImageJ software (The National Institutes of Health, Maryland, USA). Images were converted to an 8-bit gray scale and the background was subtracted. Then, binary threshold function was adjusted to obtain the highest contrast of tubules against the background. The total tubule area was calculated as the total number of pixels in images with a set threshold. Results were plotted in GraphPad Prism (GraphPad Software Inc.), where columns represent the mean values and error bars standard deviations.

4.7 Gene expression studies

4.7.1 RNA isolation

Samples for gene expression studies were collected at the 14th day of cell culture (Figure 3). Cells were lysed with the lysis buffer from Purelink RNA Minikit (Life Technologies) so that parallel sample cells from five to eight wells were lysed into 600 µl of the lysis buffer and combined as one sample. Cells were detached from the well bottom by adding the lysis buffer and scratching the well bottom with the tip of the pipette. Cell lysates were preserved at -80ºC until RNA isolation. Isolation was continued according to the instructions of the kit. RNAs were finally eluted into 35 - 40 µl of RNAse free water and the RNA concentrations and 260/280 purity ratios were measured with µPlate (Thermo Fischer) and Varioskan flash multimode reader (Thermo Fischer). Genomic

DNA contaminations were eliminated with Purelink DNAse treatment (Life Technologies). RNA samples were preserved at -80ºC until cDNA synthesis.

The possible degradation of RNA samples was studied with gel electrophoresis using QIAxcel RNA QC kit v2.0 (Qiagen, Venlo, Netherlands) and QIAxcel Advanced (Qiagen). QIAxcel RNA gel cartridge and buffer tray were prepared according to the instructions of the kit. Also samples for the run were prepared according to the instructions. Each reaction mix contained 1 µl of RNA, QX RNA size marker and QX RNA denaturation buffer, which were heated at 70 ºC for two minutes. After this, reaction mixtures were placed on ice for 1 minute and then briefly spinned. Then, 7 µl of QX RNA dilution buffer was added to each reaction mixture, after which the samples were analyzed with QIAxcel Advanced (Qiagen).

4.7.2 cDNA synthesis

From each RNA sample, complementary DNA (cDNA) was synthetized with iScript cDNA synthesis kit (Biorad, Hercules, CA, USA) according to the protocol of the manufacturer. Each reaction mixture contained 4 µl of 5x iScript reaction mix, 1 µl of iScript reverse transcriptase and RNA diluted with nuclease-free water to a final volume of 20 µl. Syntheses were conducted with CFX96 Real-Time System (Biorad) as follows: 5 min at 25ºC, 30 min at 42ºC, 5 min at 85ºC and then cooled down to 4ºC. cDNAs were then preserved at -80ºC until RT-qPCR.

4.7.3 RT-qPCR

cDNA samples were analyzed with RT-qPCR in order to evaluate differences in gene expression between the different samples. Used housekeeping genes and adipocyte marker genes are listed in Table 7.

Table 7: Used housekeeping genes and adipocyte markers.

Gene name	Abbreviation	Function
Succinate dehydrogenase complex, subunit A	SDHA	Housekeeping gene
Acidic ribosomal phosphoprotein P0	36B4	Housekeeping gene
Leptin	-	Adipose tissue secretory product
Adiponectin	-	Adipose tissue secretory product
Adipocyte protein 2	AP2	Carrier protein for fatty acids in adipose tissue
Peroxisome proliferator-activated receptor γ	PPARγ	Transcription factor in adipogenesis
Glucose transporter type 4	Glut4	Glucose transporter in adipose tissue

To ensure primer specificity, primer sequences were checked with Primer-BLAST (National Center for Biotechnology Information, Bethesda, Maryland, USA). After specificity check, primers were ordered from Oligomer Oy (Helsinki, Finland). Primer sequences, product lengths and their melting temperatures reported by the manufacturer are listed in Table 8.

Table 8: Primers used in RT-qPCR, their sequences and melting temperatures reported by the manufacturer.

Gene name	Primer sequence (5'→ 3')	Melting temperature (T_m)	Product length
SDHA	F: CATGCTGCCGTGTTCCGTGTGGG	67,8 ºC	321 bp
	R: GGACAGGGTGTGCTTCCTCCAGTGCTCC	72,4 ºC	
36B4	F: ATGCTCAACATCTCCCCCTTCTCC	64,4 ºC	251 bp
	R: GGGAAGGTGTAATCCGTCTCCACAG	66,3 ºC	
Leptin	F: GCCCTATCTTTTCTATGTCC	55,3 ºC	387 bp
	R: TCTGTGGAGTAGCCTGAAG	56,7 ºC	
Adiponectin	F: GGCCGTGATGGCAGAGAT	58,2 ºC	109 bp
	R: CCTTCAGCCCGGGTACT	57,6 ºC	
AP2	F: GCTTTTGTAGGTACCTGGAAACTT	59,3 ºC	125 bp
	R: ACACTGATGATCATGTTAGGTTTGG	59,7 ºC	
PPARγ	F: CAGTGTGAATTACAGCAAACC	55,9 ºC	101 bp
	R: ACAGTGTATCAGTGAAGGAAT	54,0 ºC	
Glut4	F: TGGGCGGCATGATTTCCTC	58,8 ºC	88 bp
	R: GCCAGGACATTGTTGACCAC	59,4 ºC	

PCR amplification was performed with CFX96 Real-Time System (Biorad) and with iQ™ SYBR® Green supermix (Biorad). Each reaction contained 25 µl of iQ™ SYBR® Green supermix, forward and reverse primers for 300nM primer concentration and 30 ng of the template, diluted with nuclease-free water to a final volume of 50 µl. Thermal cycling conditions were as follows:

1. Initial denaturation and enzyme activation — 95 ºC — 3 min
2. Denaturing — 95 ºC — 10 sec
3. Annealing — 51 - 65 ºC (gradient) — 15 sec
4. Extension — 72ºC — 30 sec
    - Steps 2. - 4. repeated 39 times
5. Melt Curve (in 0.5 ºC increments) — 55 - 95 ºC — 10 sec

Before sample runs, the annealing temperature was optimized for each primer pair. Based on the results, the annealing temperature for each primer pair was set as is represented in Table 9.

Table 9: Annealing temperatures used for each primer pair.

Row	Primer pair	Temperature
A	SDHA	65 ºC
B	36B4	64,2 ºC
D	Leptin	59,9 ºC
E	Adiponectin	56,5 ºC
F	AP2	53,8 ºC
G	PPARγ	51,9 ºC
H	Glut4	51,0 ºC

In order to monitor the size and quality of the amplified DNA, amplified DNA-samples were studied with gel electrophoresis using High Sensitivity DNA analysis kit (Agilent Technologies, Santa Clara, California, USA) and Agilent 2100 Bioanalyzer (Agilent Technologies). The chip priming station was set up according to the protocol of the manufacturer. The gel-dye mix was prepared by first pipetting 5 µl of High Sensitivity DNA dye concentrate into 100 µl of High Sensitivity DNA gel matrix. The mixture was then vortexed and spinned, after which it was loaded on the High Sensitivity DNA chip according to the protocol of the manufacturer. After that, 5 µl of High Sensitivity DNA marker, 1 µl of High Sensitivity DNA ladder and 1 µl of each sample were pipetted on the chip. After brief vortexing, the samples were analyzed with Agilent 2100 Bioanalyzer (Agilent Technologies).

qPCR data was analyzed using CFX96 Real-Time System software (Biorad). The relative quantification of each gene was calculated from the cycle threshold (Ct) values by applying the $2^{-\Delta\Delta CT}$ –method (Livak & Schmittgen, 2001). Mean fold changes were calculated with Microsoft Excel 2010 (Microsoft Corporation) with the following equation:

Fold change = $2^{-\Delta\Delta CT}$, where $\Delta\Delta Ct = \Delta Ct_{reference} - \Delta Ct_{target}$ and

where $\Delta Ct_{target} = Ct_{control} - Ct_{treatment}$ and $\Delta Ct_{reference} = Ct_{control} - Ct_{treatment}$

This way, the normalized gene expression of each target gene is compared that of the control sample. In this study, undifferentiated hASC-HUVEC co-culture samples (negative controls, see Table 6) were used as controls to indicate the extent of adipocyte differentiation. If the target gene was not detected in the sample ($Ct \geq 40$), the Ct value of 40 was used, so that the equation would

mathematically apply to the situation. In order to visualize down-regulation better, fold regulations were determined. For fold change values 1 ≥, fold regulation is equal to fold change and for fold change values <1, fold regulation is the negative inverse of fold change -1/ (fold change). 5 biological replicates of each strategy were analyzed. Fold regulation results were plotted in GraphPad Prism (GraphPad Software Inc.), where columns represent the mean values and error bars standard deviations.

4.8 Statistical analyzes

All statistical analyzes were performed with GraphPadPrism (GraphPad Software Inc.). Results from triglyceride accumulation, Cell-IQ image analysis and RT-qPCR were subjected to one-way analysis of variance (ANOVA), followed by Dunnet's multiple comparison test and Tukey's multiple comparison test. Dunnet's test compares one group with other groups and was thus used to test whether there is a difference between untreated and treated samples (i.e. negative control was compared with other samples). Tukey's test compares all the groups with each other and was used to investigate the possible difference between different strategies. Differences were considered significant when *$p<0.05$ (significant), **$p<0.01$(very significant) and ***$p<0.001$ (extremely significant).

4.8.1 Quantification of triglyceride accumulation

The significance of the differences in triglyceride accumulation between negative control and other samples was tested by one-way ANOVA with Dunnet's multiple comparison test. Fat control and different strategies were also compared with each other and the significance of the differences was tested by one-way ANOVA with Tukey's multiple comparison test. For every sample, n was 12.

4.8.2 Quantification of the area of the vascular networks

The significance of the differences in the tubule area between negative control and other samples, was tested by one-way ANOVA with Dunnet's multiple comparison test. Tubule control and different strategies were also compared with each other and the significance of the differences was tested by one-way ANOVA with Tukey's multiple comparison test. For negative control, fat control, tubule control and strategies 1 and 5, n was 15, for strategy 4, n was 6 and for strategy 6, n was 3.

4.8.3 RT-qPCR result quantification

In order to examine the significance of the differences in gene expression between different samples, all samples were compared with each other by one-way ANOVA with Tukey's multiple comparison test. For every sample, n was 5.

4.9 Good laboratory practice

The laboratory work and the documentation of the study were performed in the spirit of GLP (the OECD Principles of Good Laboratory Practice: Directive 87/18/EEC) and according to the standard operating procedures of FICAM.

5. Results

5.1 Triglyceride accumulation

5.1.1 Visualization of triglyceride accumulation in contrast to vascular networks

As Adipored (Lonza Group LTD) is a fluorescent dye, the accumulation of triglycerides can be observed with fluorescence microscopy. Adipored can be seen in red and yellow, being the brighter the more triglycerides have accumulated. Triglycerides clearly accumulated to fat control, where tubules are absent. There were a few bright red spots in negative and tubule control suggesting some triglycerides have accumulated to them as well. Triglycerides accumulated evenly also to different strategies in the presence of blood vessels. Control samples and different strategies are represented in Figure 4.

5.1.2 Quantification of triglyceride accumulation

Triglyceride accumulation in different strategies and control samples was analyzed semi-quantitatively, by calculating the ratio between the normalized Adipored values and the normalized WST-1 values. Negative control 2 (see Table 6) was used as the negative control in this analysis, as there was no significant difference between the triglyceride accumulation values for negative control 1 and negative control 2 and as the cell number in negative control 2 was higher than in negative control 1, it gave the maximum background noise possible for the negative control, leading to more reliable positive results. When comparing negative control with other samples, fat control, strategy 1 and strategy 6 accumulated significantly more triglycerides than negative control (one-way ANOVA, Dunnet's multiple comparison test). When comparing different strategies and fat control with each other, strategy 5 accumulated significantly less triglyceride than fat control (one-way ANOVA, Tukey's multiple comparison test). Strategies 2 and 3 were not included in this analysis, as there were not enough data for reliable statistical analysis. The results of the quantification of triglyceride accumulation and the statistical analysis are shown in Figure 5.

5.2 The formation of vascular networks

5.2.1 Visualization of vascular networks

Vascular networks were visualized with immunocytochemical stainings and fluorescence and confocal microscopy. The overview of vascular networks in tubule control and in different strategies (strategies 2 and 3 not included) is represented in Figure 6. Tubules formed ramified networks in tubule control and in all different strategies. Vascular networks did not form in negative controls and in fat control (data not shown).

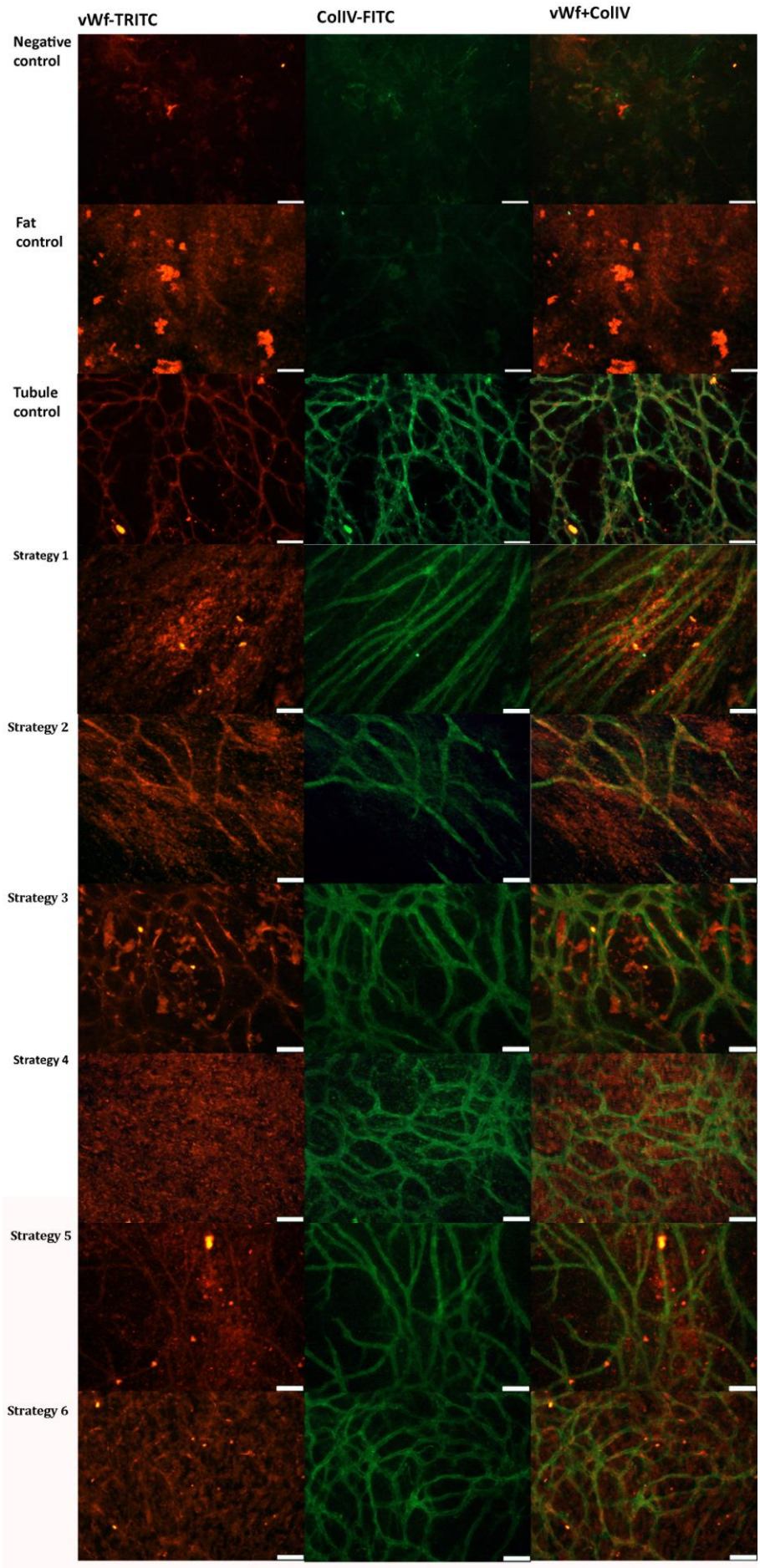

Figure 4: Triglyceride accumulation can be seen as red/yellow spots. Tubules are stained with anti-vWF and TRITC (red) and anti-ColIV and FITC (green). Images are obtained with Nikon Eclipse Ti-S inverted fluorescence microscope and with 10 x objective, scale bar is 100 µm.

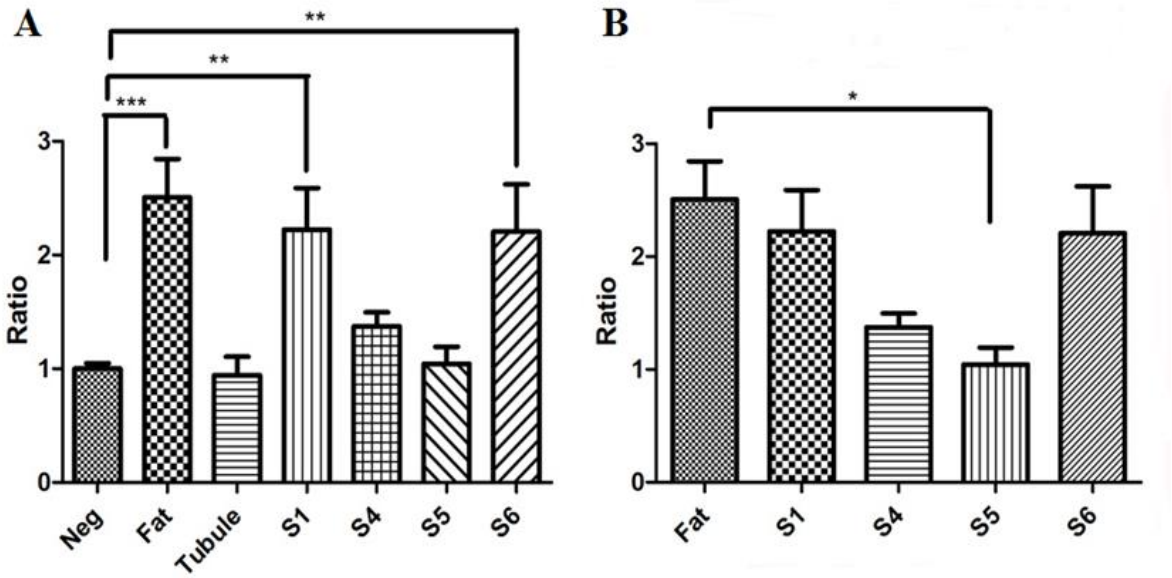

*Figure 5: Semi-quantification of triglyceride accumulation. In every sample, n=12. The bars represent mean with SD. A) Fat and tubule controls and different strategies were compared with negative control by ANOVA with Dunnet's multiple comparison test. B) Fat control and different strategies were compared with each other by ANOVA with Tukey's multiple comparison test. Differences were considered significant when *p<0.05 (significant), **p<0.01 (very significant) and ***p<0.001 (extremely significant).*

3D-structure of the formed tubules in tubule control and in all different strategies is represented in Figure 7. Inner endothelial layer (red) and the outer basement membrane (green) can be seen in all of the samples. The thicknesses of the formed vascular structures in tubule control and in different strategies did not differ markedly from each other.

5.2.2 The area analysis of vascular networks

The area of formed vascular networks was analyzed from Cell-IQ images with ImageJ. Negative control 1 was used as a negative control in this analysis, as it had the same amount of hASC as the tubule control and as there was no difference in the tubule formation between the negative samples. When comparing negative control with other samples, tubule control and strategies 1, 4, 5 and 6 had significantly more tubules than negative control (one-way ANOVA, Dunnet's multiple comparison test). When tubule control and different strategies were compared with each other, strategy 1 had significantly less tubules than tubule control and strategy 4 (one-way ANOVA, Tukey's test). Strategies 2 and 3 were not included in this analysis. The results of the vascular network area quantification and statistical analysis are represented in Figure 8.

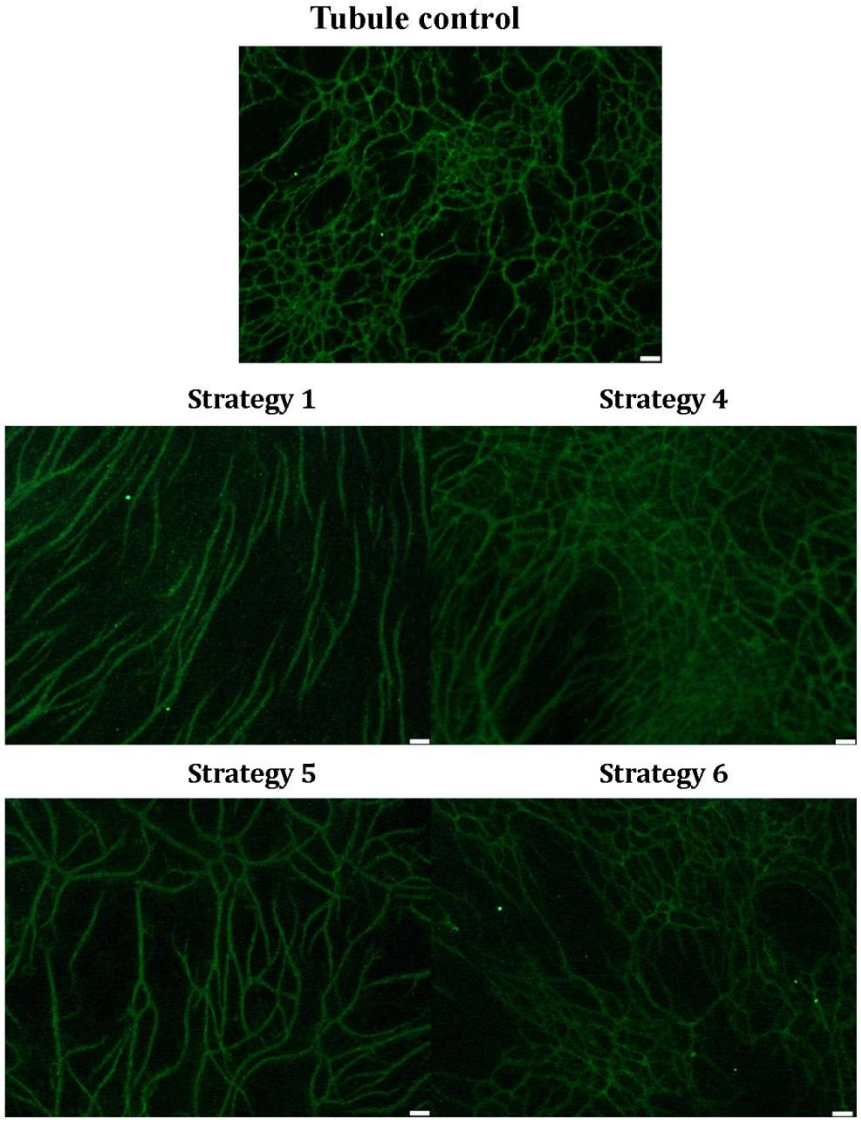

Figure 6: Overview of the vascular networks. Anti-ColIV is labeled with FITC. Images are obtained with Nikon Eclipse Ti-S inverted fluorescence microscope and with 4 x objective, scale bar is 100 µm.

5.3 The genetic profile of the formed adipose tissue

The maturation of adipose tissue was evaluated with adipose tissue specific marker genes. Expression of marker genes was studied at one time point, at the 14th day of cell culture. All data was normalized using the expression levels of SDHA, as SDHA was more stable than the other housekeeping gene, 36B4. For fat control and for strategies 5 and 6, negative control 1 was used as the calibrator, as it had the same amount of hASC and correspondingly, for strategies 1 and 4, negative control 2 was used as the calibrator. The gene expression was considered elevated when fold regulation was higher than 2. Correspondingly, gene expression was considered decreased when fold regulation was lower than -2.

The expression of PPARγ was elevated in fat control and all of the strategies, except of strategy 4, where PPARγ expression was decreased. The expression of leptin was elevated in all samples. The

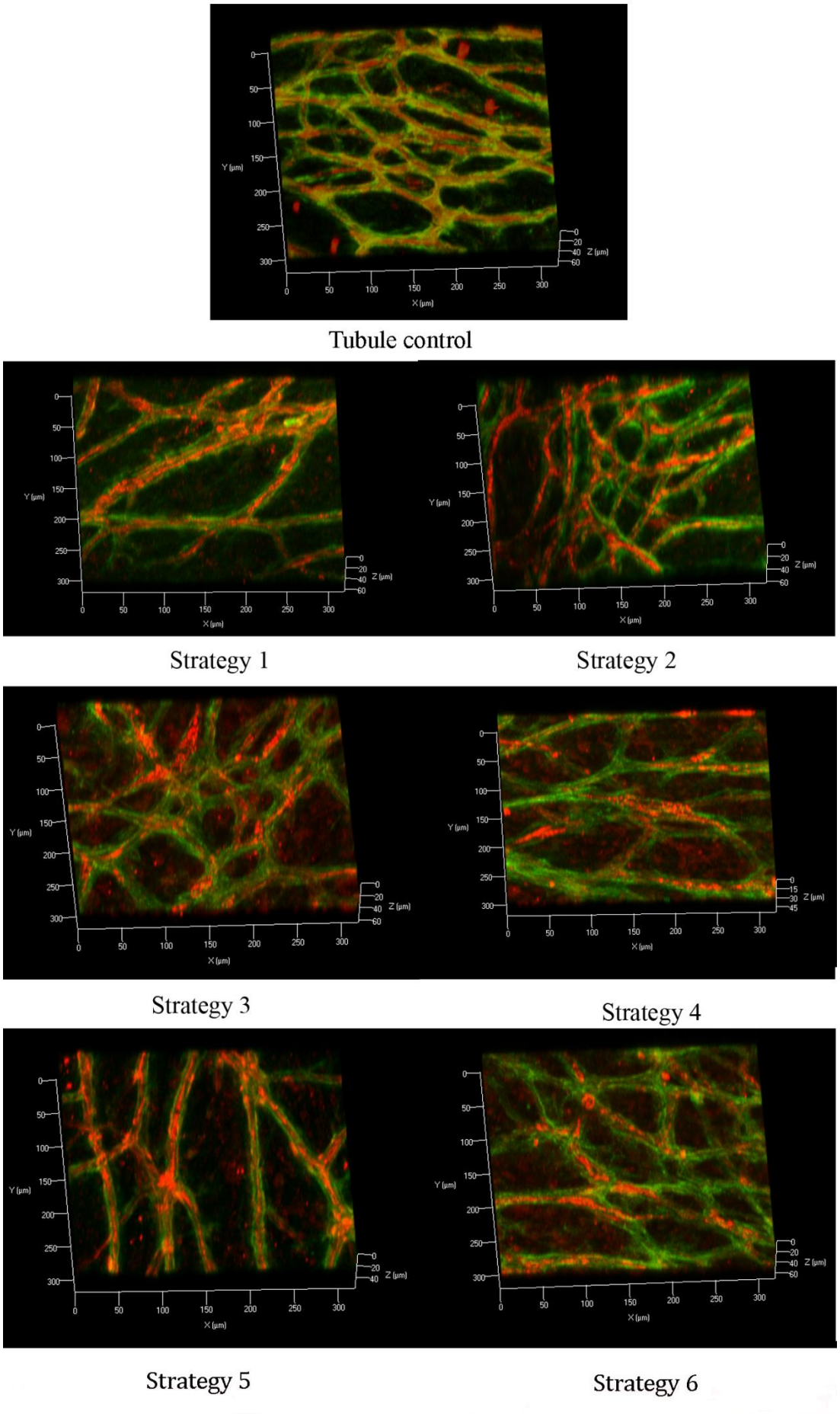

Figure 7: Visualization of the 3D-structures of the vascular networks in tubule control and in all different strategies. Anti-vWf is labeled with TRITC (red) and anti-ColIV with FITC (green). Images are obtained with LSM710 confocal microscope with 20 x objective. Scale bars are in micrometers.

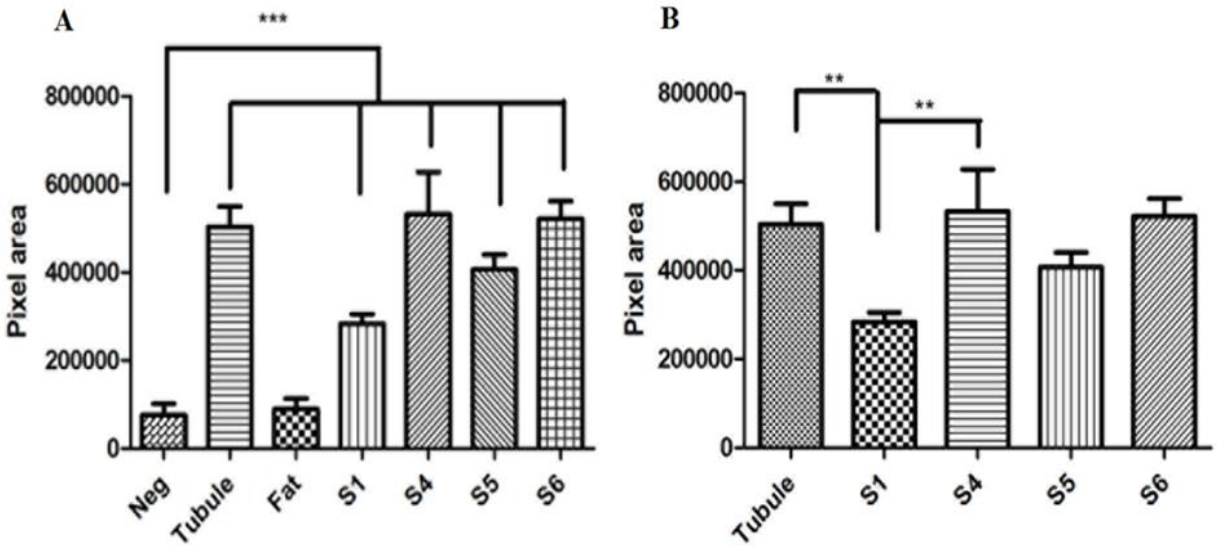

*Figure 8: The quantification of the area of tubular networks. In samples Neg, Tubule, Fat, S1 and S5, n=15. In samples S4, n=6 and in sample S6, n=3. The bars represent mean with SD.A) Tubule control, fat control and different strategies were compared with negative control by ANOVA with Dunnet's multiple comparison test. B) Tubule control and different strategies were compared with each other by ANOVA with Tukey's Multiple comparison test. Differences were considered significant when *p<0.05 (significant), **p<0.01 (very significant) and ***p<0.001(extremely significant).*

expression of adiponectin was elevated in fat control and in strategies 4,5 and 6. AP2 expression was decreased in fat control and in strategies 4 and 6. The expression of Glut4 was elevated in fat control and in strategies 1, 5 and 6.

In order to find out the possible statistical differences in gene expression between different strategies, fat control and different strategies were compared with each other by one-way ANOVA (Tukey's multiple comparison test). There was statistical difference only in adiponectin expression: adiponectin expression was significantly more elevated in strategy 5 than in other samples. The gene expression charts and mean fold regulation values are represented in *Figure 9*.

5.3.1 Quality control & primer optimization for gene expression studies

The integrity of the isolated RNA samples was controlled along the study. Also the size and quality of the amplified DNA was checked. Overall, RNA stayed intact during the isolation and DNA product of right size was amplified. A quality control panel with example samples is represented in Figure 10. In order to achieve maximal amplification for each gene, annealing temperatures for each primer pair were optimized. Annealing temperatures were selected based on the lowest C_T value and melt curve analysis. An example of melting curve analysis is represented in Figure 10.

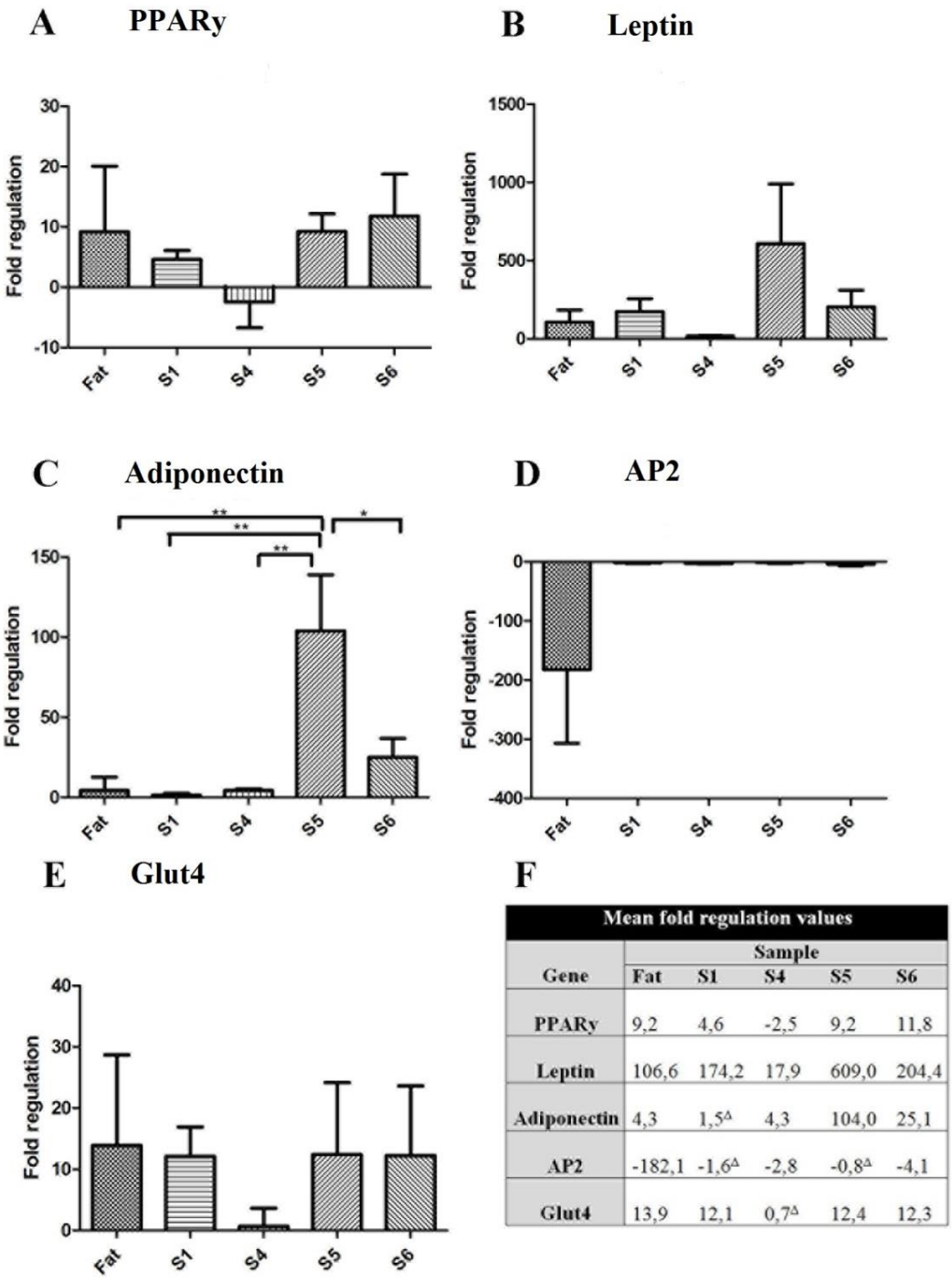

F

Mean fold regulation values					
Gene	Sample				
	Fat	S1	S4	S5	S6
PPARy	9,2	4,6	-2,5	9,2	11,8
Leptin	106,6	174,2	17,9	609,0	204,4
Adiponectin	4,3	1,5$^{\Delta}$	4,3	104,0	25,1
AP2	-182,1	-1,6$^{\Delta}$	-2,8	-0,8$^{\Delta}$	-4,1
Glut4	13,9	12,1	0,7$^{\Delta}$	12,4	12,3

*Figure 9: The gene expression of adipose tissue specific gene markers. The bars represent mean with SD. A) PPARγ B) Leptin C) Adiponectin D) AP2 E) Glut4 A-E) all samples of each gene were compared with each other by ANOVA with Tukeys multiple comparison test. F) Mean fold regulation values for each sample and gene. Values marked with Δ are neither elevated nor decreased. Differences were considered significant when *p<0.05 (significant), **p<0.01(very significant) and ***p<0.001 (extremely significant).*

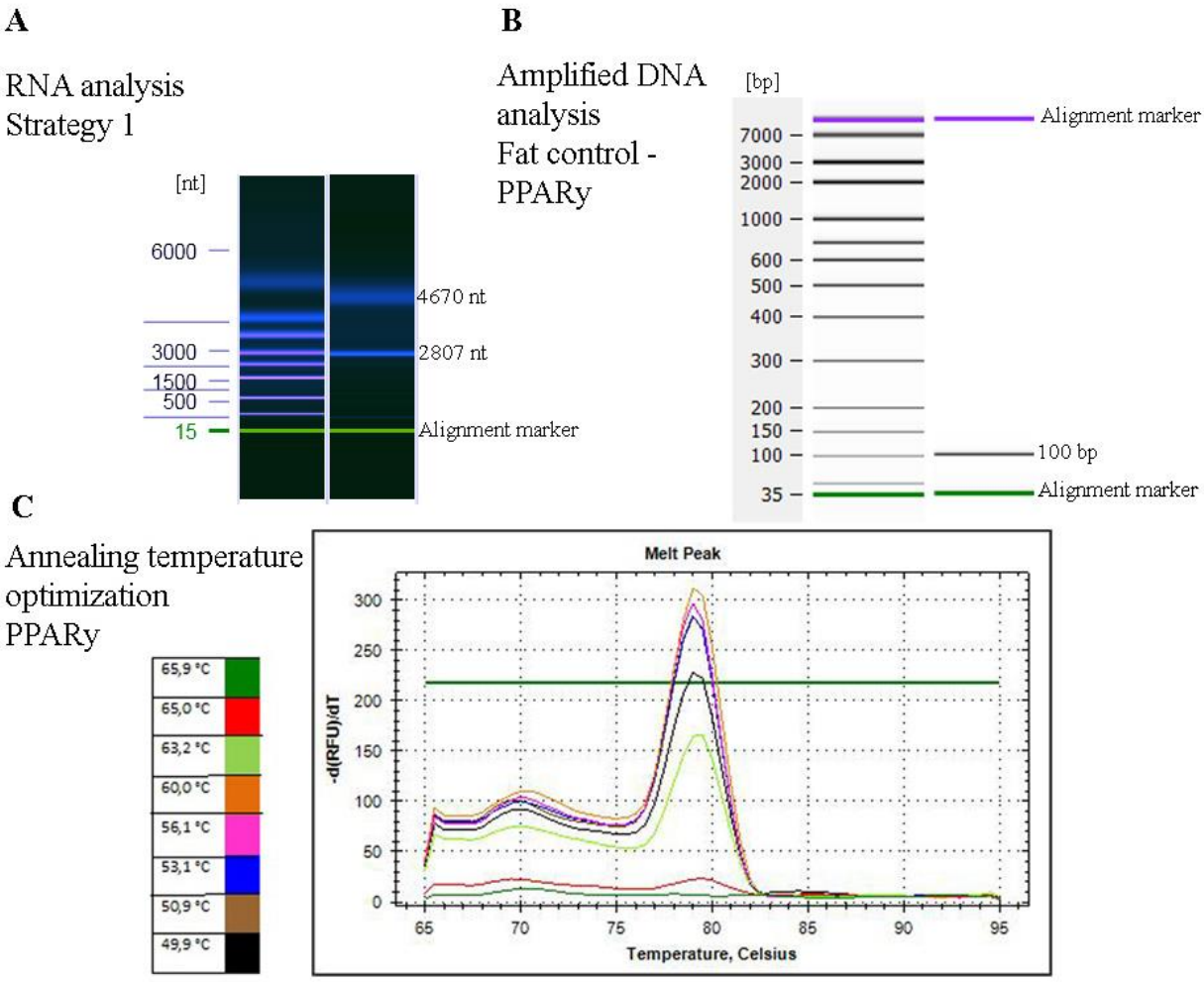

Figure 10: Primer optimization & quality control panel. A) RNA analysis for detecting possible decomposition. The RNA ladder is presented on the left and sample line on the right. On the sample line, the visible bands of the sizes 2807 and 4670 nucleotides are both ribosomal-RNA. As the two bands can be detected, RNA is not decompiled. B) Analysis for amplified DNA. The DNA ladder is presented on the left and sample line on the right. The band on the sample line size of 100 bp is the amplified DNA. The product size of PPARγ according to Primer-BLAST is 101 bp. C) Annealing temperature optimization for primer pairs. Sharp and high peak suggests that there is a single amplicon. Temperatures from 50.9°C to 60.0°C degrees would work for this primer pair. 51.9°C degrees was selected for the annealing temperature for PPARγ.

6. Discussion

In this study, different cell culturing strategies were tested, in order to form a functional vascularized adipose tissue model by combining ATE-induced adipogenesis of hASC culture to the blood vessel structures formed in hASC-HUVEC angiogenesis model. ATE-induced adipogenesis of hASC cultures has been proven before (Sarkanen et al., 2012a) and a hASC-HUVEC based angiogenesis model has been optimized before (Huttala et al., 2015; Sarkanen et al., 2012b). Overall, adipose tissue and blood vessels were both formed with all of the strategies, although there were differences in triglyceride accumulation and in the density of vascular networks in different strategies. Most of the adipose tissue specific genes' expressions were elevated in adipose tissue formed with all the strategies. Results showed that strategy 1, where adipose tissue was induced before blood vessels and cells were plated in two batches at two different days, was technically the best strategy for solving the detachment issue frequently seen in multilayered cell cultures, accumulated adequate amount of triglycerides, expressed adipose tissue specific genes and the morphology of adipocytes and blood vessels was similar to their morphology *in vivo*.

6.1 Cell detachment issues

Earlier attempts to combine ATE-induced adipogenesis of hASC culture to angiogenesis model have faced severe cell detachment issues. One aspect for testing different cell culturing strategies (Table 5) was thus to find out if the cell detachment problem could be solved by changing the plating or the differentiation scheme.

In strategies 2 and 3 cells started to detach from the bottom of cell culture plate already after 2 - 3 days, probably because of the great cell number plated already on the first day. Strategies 5 and 6 were other ways identical to strategies 2 and 3, in respect, but the number of hASC used in strategies 5 and 6 was only half of the cell number used in strategies 2 and 3. Because of the detachment issues, strategies 2 and 3 were not tested further and were thus not included in most of the analysis.

Although the best strategy was chosen based on the quantitative data obtained from different analysis, also the hands-on experience of cell culturing had importance. In addition to strategies 2 and 3, also other strategies had some detachment issues. However, in other strategies the possible detachments occurred on the 11^{th} to 14^{th} day of cell culturing, i.e. much later than in strategies 2 and 3. Thus, adipose tissue and blood vessels had already formed in most cases. In strategies 4 and 6, where blood vessels were induced before adipose tissue, the detachment was more frequent than in strategies 1 and 5, where adipose tissue was induced before blood vessels. Thus, it seems that

differentiation order has an effect on the cell detachment issue. Differentiating adipose tissue before blood vessels seems to be the best differentiating order for the cell adherence.

Cell detachment occurred in most detachment cases so that the uppermost cell layers of the cell mat started to bud from the edges of the cell culturing well. In the worst cases, the cell mat formed a cell ball at the bottom of the cell culturing well. Cells inside the cell ball might not be as viable as the cells on the outer surface of the cell ball and the cells growing as they were intended to, planar. Detachment of cells in tissue models is a serious problem when considering the applicability and reliability of the model. For instance, if the vascularized adipose tissue model would be used in chemical testing, it is important that the morphology of adipocytes and blood vessels can be seen. Detection of the possible effect of the chemical on the adipogenesis and/or angiogenesis would be impossible if the cells detached.

6.2 Triglyceride accumulation

Mature adipocytes contain microscopic intracellular lipid droplets that are the first visible signs of adipose tissue formation (J. H. Choi et al., 2010). Triglycerides accumulated to all the different strategies forming visible lipid droplets, regardless of the differentiation order or the plating scheme. However, only the accumulation obtained with strategies 1 and 6 was statistically significantly greater than in the negative control (Figure 5A). When fat control and different strategies were compared with each other, there was a significant statistical difference only between fat control and strategy 5 (Figure 5B).

In strategy 1, adipose tissue was induced before blood vessels and in strategy 6, blood vessels before adipose tissue. In strategy 1, hASC and HUVEC were added in between differentiations and in strategy 6, all the cells were plated at the beginning of cell culture. Strategy 6 included only half of the number of hASC compared with strategy 1. As strategies 1 and 6 are different cell culturing schemes in respect to differentiation order, cell plating and hASC number, it is possible that these variables in the cell culturing set-up do not have an effect on triglyceride accumulation.

Adipored-treated cell cultures were imaged with fluorescent microscopy to observe adipocyte morphology. Adipored-treated cell cultures were also double-stained with blood vessels specific antibodies vWf and ColIV, which were labeled with TRITC and FITC, in respect (Figure 4). This way triglyceride accumulation in contrast to blood vessel formation could be seen although TRITC and Adipored can be seen partly in the same color. Based on the fluorescence images, triglycerides were present in fat control and all the different strategy samples. According to the images, triglyceride accumulation was not disturbed even though vascular networks were formed with

different strategies. Although negative control and tubule control were not treated with ATE, some triglycerides still accumulated, based on both absorbance measurements and fluorescence images. hASC include also committed preadipocytes, which are already determined to become adipocytes (Gregoire, 2001), which could explain the occurrence. However, without ATE-treatment, accumulation of triglycerides barely existed.

Triglyceride accumulation to hASC-HUVEC based vascularized adipose tissue models has been proven also by others (Kang et al., 2009; Wittmann et al., 2015). In the model of Kang *et al*., the adipogenic inducement was achieved with an adipogenic cocktail, which included insulin, IBMX, biotin, pantothenate, DEX and thiazolidinediones (Kang et al., 2009). Wittmann *et al*. used insulin, IBMX, DEX and indomethacin containing adipogenic cocktail (Wittmann et al., 2015). However, as mentioned before, ATE is proven to induce accelerated and higher triglyceride accumulation, when compared with a standard adipogenic cocktail including insulin, IBMX, DEX and indomethacin (Sarkanen et al., 2012a).

6.3 The formation of vascular networks

Vascular networks were formed successfully with all the different cell culturing strategies. Confocal microscope images showed that tubules formed in tubule control and in all strategies have similar structure: the inner endothelial layer is covered with the basement membrane just like in real capillaries in the body. Formed vascular networks were about the same thickness in the tubule control and in different strategies. Based on the confocal images, also the vertical diameter of the formed capillaries and the thickness of the basement membrane seem similar in tubule control and in different strategies.

When observing the vascular network images taken with a fluorescent microscope and with 4 x objective, one can see that ramified vascular networks were formed with all of the strategies, but it seems that in tubule control and in strategies 4 and 6 networks were denser than in strategies 1 and 5. Quantitative tubule area analysis from Cell-IQ images showed that tubule control and all the strategies had significantly more tubules than negative control (Figure 8A). When comparing tubule control and different strategies with each other, only strategy 1 had significantly less tubules than tubule control and strategy 4 (Figure 5B). However, n for strategies 4 (n=6) and 6 (n=3) was considerably smaller than for other samples (n=15). Thus, there would probably have been a statistical difference between strategy 6 and strategy 1 as well, if n for strategy 6 would have been greater.

As blood vessels were induced first in strategies 4 and 6, it is logical that denser vascular networks occurred. In these strategies, blood vessels had time to mature for 14 days. On the other hand, in strategies 1 and 5, where adipose tissue was induced first, blood vessels were able to mature only for 7 days, which results in less dense vascular networks. However, in pre-validated angiogenesis model, the maturation time for blood vessels is also 7 days (Sarkanen et al., 2012b). Although vascular networks were not as dense in strategies 1 and 5 as they were in strategies 4 and 6, they were still ramified and had similar structure, where the basement membrane and the endothelial cells could be seen. Thus, for this purpose, vascular networks induced by strategies 1 and 5 are as appropriate as vascular networks induced by strategies 4 and 6.

Although blood vessels were induced with angiogenesis stimulation medium, the vascularized adipose tissue co-cultures were also treated with ATE, which in addition to adipogenesis induces angiogenesis (Sarkanen et al., 2012a). Thus, it is possible that ATE treatment further enhances blood vessel maturation. ATE-treatment alone did not normally induce dense vascular network formation, as was seen from fat control. However, ATE treatment does not seem to disturb vascular network formation. In other vascularized adipose tissue models, adipogenic cocktail treatments have been suspected to have a negative effect on endothelial cells and delay HUVEC growth (Foley et al., 2015; Kang et al., 2009).

6.4 The genetic profile of the formed adipose tissue

Based on the RT-qPCR results, adipogenesis occurred at least to some extent in fat control and in all the different strategies. The studied gene markers were PPARγ, leptin, adiponectin, Glut4 and AP2, which are all commonly used adipogenesis markers (J. H. Choi et al., 2010). Overall, the expression of PPARγ, leptin, adiponectin and Glut4 was elevated and the expression of AP2 was decreased in most samples.

When looking at the results in more detail (Figure 9), fat control and strategy 6 have similar expression: PPARγ, leptin, adiponectin and Glut4 expressions are elevated and AP2 expression is decreased. The gene expression in strategy 5 is other ways similar, except that AP2 expression is not decreased. The expression of strategy 1 in turn resembles strategy 5, except that adiponectin expression is not elevated. In strategy 4, only leptin and adiponectin expressions are elevated, whereas the expression of PPARγ and AP2 is decreased. Glut4 expression is neither elevated nor decreased.

There were 5 biological replicates in this study. Overall, 3 different hASC-HUVEC combinations and 6 different ATE batches were used. This causes some natural dispersion on the results, as the

cells and ATE are isolated from different donors. This also partly explains why the standard deviations for some similarly treated samples, e.g. strategy 5-leptin, strategy 5-adiponectin and fat control-AP2 were high. Another explanation for the dispersion may come from ATE-treatment itself: in addition to adipogenesis and angiogenesis, ATE induces proliferation (Sarkanen et al., 2012a). Thus, in the ATE-treated cell cultures, there are preadipocytes and adipocytes in many different developmental phases and all of the cells do not have enough time to mature into adipocytes. In both fat control and strategy 5, all cells are plated at once, at the beginning of cell culture. Fat control is treated only with ATE, whereas strategy 5 is treated the first 7 days with ATE and then the remaining 7 days with angiogenesis stimulation medium. In strategy 5, adipocytes can thus mature for the entire cell culturing time. However, as the medium changes from ATE to angiogenesis stimulation medium after one week, it is possible that the already more maturated adipocytes, committed preadipocytes, continue maturation during the angiogenesis stimulation medium treatment whereas early stage preadipocytes, which would still need adipogenic cues that ATE offers, stay at their developmental phase. Angiogenesis stimulation medium is serum free, so it enhances the differentiation of the cells at the expense of proliferation. Thus, angiogenesis stimulation medium might enhance the differentiation of the committed preadipocytes.

Elevated PPARγ expression in fat control and in all of the different strategies, except of strategy 4, suggests that adipogenesis has begun. In 3T3-L1 cells, PPARγ expression rises rapidly after the hormonal induction of differentiation and maximum expression is attained in mature adipocytes (Gregoire et al., 1998). Elevated PPARγ expression has been detected also in hASC based obesogen screening model (Foley et al., 2015). The results for strategy 4 are controversial, as the decreased expression of PPARγ would suggest that adipogenesis does not occur, leptin and adiponectin expressions are still elevated.

Leptin and adiponectin are the most abundant secretory products of adipose tissue (Coelho et al., 2013). The expression of leptin and adiponectin is thus typically investigated, when studying the secretory properties of the formed adipose tissue (J. H. Choi et al., 2010). The expression of leptin was elevated in all of the samples which implies to functional adipose tissue formation. However, the protein expression of the formed adipose tissue needs yet to be confirmed. In 3T3-L1 cells, the gene and protein expression of leptin is elevated during the terminal differentiation of adipocytes, being however much lower than that detected in native adipose tissue (Gregoire et al., 1998). Leptin secretion has been studied also in hASC-HUVEC based vascularized adipose tissue: leptin secretion was detected to be higher in samples that were treated with adipogenic cocktail when compared with untreated samples (Kang et al., 2009).

Also adiponectin expression results suggest that functional adipose tissue has formed: the expression of adiponectin was elevated in fat control and all the strategies except of strategy 1. Also in 3T3-L1 cells, adiponectin gene and protein expression is elevated (Gregoire et al., 1998). When the samples were compared with each other, there was statistically significant difference in adiponectin expression: in strategy 5 adiponectin expression was elevated significantly more than in other samples. However, the expression of adiponectin was generally low, with C_T values higher than 35, so the fold regulation values calculated with these results are not that reliable.

Glut4 is a glucose transporter that is translocated by insulin to adipocyte cell surface in high-fed state (Watson & Pessin, 2007). Glut4 expression thus describes the metabolic state of the formed adipose tissue. Glut4 expression was elevated in all the samples, however, as it was with adiponectin, the general expression of Glut4 was also low (C_T values>35). The fold regulation values are thus not that reliable. In 3T3-L1 cells, the expression of Glut4 rises in the terminal stage of differentiation (Gregoire et al., 1998).

AP2, also known as fatty acid-binding protein 4, belongs to lipid chaperon protein family that regulate the lipid trafficking and response in cells (Furuhashi et al., 2015). The expression of AP2 was decreased in fat control and in strategies 4 and 6. In strategies 1 and 5, AP2 expression was neither elevated nor decreased. Although there was no statistical difference in AP2 expression between different samples, it is interesting that AP2 expression seems to be less or not at all decreased in different strategies, whereas in fat control AP2 expression is clearly decreased. As angiogenesis stimulation medium includes insulin, which increases glucose influx and represses lipolysis in adipocytes (S. M. Choi et al., 2010; Watson & Pessin, 2007), it is possible that the combination of ATE and angiogenesis media treatments enhances adipose tissue maturation more than just ATE treatment. It is also possible, that formed vasculature supports adipocyte maturation, as activated endothelial cells in angiogenic vessels are known to produce various cytokines and growth factors that promote adipose tissue growth and expansion (H. Cao, 2014). However, more studies are needed to confirm the effect of angiogenesis stimulation medium and vascularization on the maturity of the formed adipose tissue.

Studies with 3T3-L1 cell line have shown that AP2 expression rises during the terminal stage of differentiation (Gregoire et al., 1998). Thus, it is possible that the formed adipose tissue has not entirely matured. Generally low adiponectin and Glut4 gene expressions would support this theory. Preadipocyte cell lines are already committed to adipocyte cell line and are thus further in development than hASC, which could explain the difference. However AP2 expression has been

detected to be elevated also in the hASC based obesogen screening model (Foley et al., 2015), when treated with an adipogenic cocktail including insulin, IBMX, DEX and rosiglitazone. Foley *et al*. assessed the relative gene expression using the $2^{-\Delta\Delta CT}$ method and GAPDH as the housekeeping gene. However, although GAPDH is one of the most used housekeeping genes, it has been detected to be regulated during dietary intervention (Viguerie et al., 2012). Thus, it is not the most ideal housekeeping gene for adipose tissue studies and may skew the fold regulation value results.

6.5 The vascularized adipose tissue model built with strategy 1 showed the most promising results

When considering the best cell culturing strategy for building the vascularized adipose tissue model, strategies 1 and 6 showed the most promising quantitative data. Triglycerides were accumulated, a sufficient vascular network was formed and adipocyte specific genes were expressed. However, strategy 6 had more serious detachment issues than strategy 1, so strategy 1 should be selected for further development of human vascularized adipose tissue.

In strategy 6, blood vessels were induced before adipose tissue and all the cells were plated on the day 0 (Figure 3). Blood vessels had 14 days long maturation time and formed thus quite dense blood vessel networks. It might be that dense and mature blood vessel network would support the maturation of adipose tissue. The RT-qPCR results of AP2 would support this theory. However, in strategy 4, which also had a dense blood vessel network, adipose tissue did not significantly mature. The difference between strategies 6 and 4 was, that in strategy 4, cells were plated on two days (day 0: hASC and HUVEC, day 7: hASC) and that the total hASC number used in strategy 4 was twice as high when compared with strategy 6. Thus it is possible that the good maturation of adipocytes in strategy 6 results of the positive effect of angiogenesis stimulation medium on adipogenesis.

In strategy 1, adipose tissue was induced before blood vessels and cells were plated on day 0 (hASC) and on day 7 (hASC and HUVEC) (Figure 3). Adipose tissue had thus long maturation time, which would explain why adipose tissue maturated so well. However, also in strategy 5, adipose tissue was induced before blood vessels having thus the same maturation time for adipose tissue, but adipose tissue did not seem to mature based on the triglyceride accumulation. The difference between strategies 5 and 1 was that in strategy 5, all the cells were plated on the day 0 and that the total hASC number used in strategy 1 was twice as high when compared with strategy 5. On the other hand, the RT-qPCR results for strategy 5 would suggest that the formed adipose tissue is mature. The maturity of the adipose tissue formed with strategy 5 thus remains questionable. Overall, it seems that inducing adipose tissue before blood vessels would be beneficial for adipose tissue maturation.

6.6 The future of vascularized adipose tissue

Although strategy 1 should be chosen for further development, the good results obtained with strategy 6, which had only half of the hASC number of strategy 1, give reason to question the necessity of hASC addition in the second batch in strategy 1. If as good triglyceride accumulation, vascular network formation and adipogenesis specific gene expression could be achieved by leaving the second batch of hASC out, the model would be more cost-effective, as hASC number and needed working hours would decrease. Thus, this kind of plating strategy would yet be worth testing.

In addition to plating strategy refinement, as the gene expressions of some of the adipogenesis specific gene markers were low or in the case of AP2, not elevated at all, adipocyte maturation could be enhanced. In order to maturate the formed adipose tissue further, the composition of ATE medium could be optimized. Insulin addition would perhaps come into the question. However insulin concentration should be lower than in commonly used adipogenic cocktails, which use supraphysiological concentrations (Gregoire, 2001). Normal insulin concentrations would keep the vascularized adipose tissue model closer to the normal body conditions and preserve the insulin sensitivity of the model. Also the effect of serum free ATE medium to the model differentiation could be tested.

Blood vessels formed by every strategy had similar structure: TRITC labeled endothelial cells were covered by FITC labeled basement membrane. However, in addition to the endothelial cells and the basement membrane, real capillaries in the body have pericyte layer that loosely covers the basement membrane (Szoke et al., 2012). Thus, pericyte staining would ensure the authentic structure. It would also be interesting to find out the existence of lumen with electron microscopy.

Immunocytochemical stainings could also be used in order to study more closely the morphology of the formed adipose tissue. Collagen VI is the major protein in adipose tissue ECM (Divoux & Clement, 2011) and would thus be suitable for this purpose. Also staining CD36, which is needed in the transportation process of fatty acids into adipocytes (Rutkowski et al., 2015), could provide useful information about the composition of the formed adipocytes.

The next thing in the model optimization would be the examination of protein secretion of the model. As it seems that leptin and adiponectin mRNAs are expressed, their protein expression should also be ensured. In order to investigate the metabolic functionality of the formed adipose tissue, the effectiveness of lipolysis and the insulin sensitivity of the model should be studied. After optimization, the vascularized adipose tissue model will be tested with reference chemicals that

have well-established effect on adipogenesis and/or angiogenesis. After the chemical testing, the model is ready for intra-laboratory validation.

The vascularized adipose tissue model optimized in this study could also fit interesting applications in the field of tissue-engineering. hASC and endothelial cell based vascularized adipose tissue has been successfully grown by others *in vitro* and/or *in vivo* on 3D silk scaffolds and in fibrin gels (Borges et al., 2003; Kang et al., 2009; Wittmann et al., 2015). Thus, it is plausible that our model could also be grown on biomaterials. The advantages that our model has over to the existing vascularized adipose tissue models are the novel and own differentiation media, ATE medium and angiogenesis stimulation medium.

7. Conclusions

In this study, the hASC-HUVEC based human vascularized adipose tissue model was optimized and characterized in respect of cell plating and differentiation scheme. The results showed, that changing the cell plating and differentiation schemes affected the technical repeatability and reliability of the model, triglyceride accumulation, vascular network formation and the genetic maturity of the formed adipose tissue. A scheme, which showed the best results with respect to these variables, was selected to be further developed.

Maturation of adipocytes might be enhanced in the presence of blood vessels although more experiments are needed to confirm this. However, it is clear that proper vascular structures can be formed in the presence of adipocytes and that the cell plating and differentiation scheme have a notable effect on the technical repeatability and reliability of the model.

The vascularized adipose tissue model is a promising tool for adipose tissue research. By thorough characterizing and optimizing the formed *in vitro* model, it is possible to create a more accurate, reliable and efficient test system than the currently available animal models offer.

8. References

Abel, E. D., Peroni, O., Kim, J. K., Kim, Y. B., Boss, O., Hadro, E., Minnemann, T., Shulman, G. I., & Kahn, B. B. (2001). Adipose-selective targeting of the GLUT4 gene impairs insulin action in muscle and liver. *Nature, 409*(6821), 729-733.

Ahmed, K., Tunaru, S., Tang, C., Muller, M., Gille, A., Sassmann, A., Hanson, J., & Offermanns, S. (2010). An autocrine lactate loop mediates insulin-dependent inhibition of lipolysis through GPR81. *Cell Metabolism, 11*(4), 311-319.

Armani, A., Mammi, C., Marzolla, V., Calanchini, M., Antelmi, A., Rosano, G. M., Fabbri, A., & Caprio, M. (2010). Cellular models for understanding adipogenesis, adipose dysfunction, and obesity. *Journal of Cellular Biochemistry, 110*(3), 564-572.

Baer, P. C. (2014). Adipose-derived mesenchymal stromal/stem cells: An update on their phenotype in vivo and in vitro. *World Journal of Stem Cells, 6*(3), 256-265.

Bell, L. N., Cai, L., Johnstone, B. H., Traktuev, D. O., March, K. L., & Considine, R. V. (2008). A central role for hepatocyte growth factor in adipose tissue angiogenesis. *American Journal of Physiology.Endocrinology and Metabolism, 294*(2), E336-44.

Bergen, W. G., & Mersmann, H. J. (2005). Comparative aspects of lipid metabolism: Impact on contemporary research and use of animal models. *The Journal of Nutrition, 135*(11), 2499-2502.

Bluher, M. (2005). Transgenic animal models for the study of adipose tissue biology. *Best Practice & Research.Clinical Endocrinology & Metabolism, 19*(4), 605-623.

Borges, J., Mueller, M. C., Padron, N. T., Tegtmeier, F., Lang, E. M., & Stark, G. B. (2003). Engineered adipose tissue supplied by functional microvessels. *Tissue Engineering, 9*(6), 1263-1270.

Borges, J., Muller, M. C., Momeni, A., Stark, G. B., & Torio-Padron, N. (2007). In vitro analysis of the interactions between preadipocytes and endothelial cells in a 3D fibrin matrix. *Minimally Invasive Therapy & Allied Technologies, 16*(3), 141-148.

Bost, F., Aouadi, M., Caron, L., & Binetruy, B. (2005). The role of MAPKs in adipocyte differentiation and obesity. *Biochimie, 87*(1), 51-56.

Brasaemle, D. L., & Wolins, N. E. (2012). Packaging of fat: An evolving model of lipid droplet assembly and expansion. *The Journal of Biological Chemistry, 287*(4), 2273-2279.

Bucky, L. P., & Percec, I. (2008). The science of autologous fat grafting: Views on current and future approaches to neoadipogenesis. *Aesthetic Surgery Journal, 28*(3), 313-21.

Buettner, R., Scholmerich, J., & Bollheimer, L. C. (2007). High-fat diets: Modeling the metabolic disorders of human obesity in rodents. *Obesity, 15*(4), 798-808.

Burke, S., Nagajyothi, F., Thi, M. M., Hanani, M., Scherer, P. E., Tanowitz, H. B., & Spray, D. C. (2014). Adipocytes in both brown and white adipose tissue of adult mice are functionally connected via gap junctions: Implications for chagas disease. *Microbes and Infection, 16*(11), 893-901.

Cai, X., Lin, Y., Hauschka, P. V., & Grottkau, B. E. (2011). Adipose stem cells originate from perivascular cells. *Biology of the Cell, 103*(9), 435-447.

Cao, H. (2014). Adipocytokines in obesity and metabolic disease. *The Journal of Endocrinology, 220*(2), T47-59.

Cao, Y. (2010). Adipose tissue angiogenesis as a therapeutic target for obesity and metabolic diseases. *Nature Reviews.Drug Discovery, 9*(2), 107-115.

Cao, Y. (2013). Angiogenesis and vascular functions in modulation of obesity, adipose metabolism, and insulin sensitivity. *Cell Metabolism, 18*(4), 478-489.

Cao, Y. (2014). Angiogenesis as a therapeutic target for obesity and metabolic diseases. *Chemical Immunology and Allergy, 99*(1), 170-179.

Carmeliet, P., & Jain, R. K. (2011). Molecular mechanisms and clinical applications of angiogenesis. *Nature, 473*(7347), 298-307.

Chandrasekera, P. C., & Pippin, J. J. (2014). Of rodents and men: Species-specific glucose regulation and type 2 diabetes research. *Altex, 31*(2), 157-176.

Choi, J. H., Gimble, J. M., Lee, K., Marra, K. G., Rubin, J. P., Yoo, J. J., Vunjak-Novakovic, G., & Kaplan, D. L. (2010). Adipose tissue engineering for soft tissue regeneration. *Tissue Engineering.Part B, Reviews, 16*(4), 413-426.

Choi, S. M., Tucker, D. F., Gross, D. N., Easton, R. M., DiPilato, L. M., Dean, A. S., Monks, B. R., & Birnbaum, M. J. (2010). Insulin regulates adipocyte lipolysis via an akt-independent signaling pathway. *Molecular and Cellular Biology, 30*(21), 5009-5020.

Christiaens, V., & Lijnen, H. R. (2010). Angiogenesis and development of adipose tissue. *Molecular & Cellular Endocrinology, 318*(1-2), 2-9.

Chun, T. H., Hotary, K. B., Sabeh, F., Saltiel, A. R., Allen, E. D., & Weiss, S. J. (2006). A pericellular collagenase directs the 3-dimensional development of white adipose tissue. *Cell, 125*(3), 577-591.

Clapp, C., Thebault, S., Jeziorski, M. C., & Martinez De La Escalera, G. (2009). Peptide hormone regulation of angiogenesis. *Physiological Reviews, 89*(4), 1177-1215.

Coelho, M., Oliveira, T., & Fernandes, R. (2013). Biochemistry of adipose tissue: An endocrine organ. *Archives of Medical Science, 9*(2), 191-200.

Corvera, S., & Gealekman, O. (2014). Adipose tissue angiogenesis: Impact on obesity and type-2 diabetes. *Biochimica Et Biophysica Acta, 1842*(3), 463-472.

Cristancho, A. G., & Lazar, M. A. (2011). Forming functional fat: A growing understanding of adipocyte differentiation. *Nature Reviews.Molecular Cell Biology, 12*(11), 722-734.

Daquinag, A. C., Zhang, Y., & Kolonin, M. G. (2011). Vascular targeting of adipose tissue as an anti-obesity approach. *Trends in Pharmacological Sciences, 32*(5), 300-307.

Divoux, A., & Clement, K. (2011). Architecture and the extracellular matrix: The still unappreciated components of the adipose tissue. *Obesity Reviews: An Official Journal of the International Association for the Study of Obesity, 12*(5), e494-503.

Farmer, S. R. (2005). Regulation of PPARgamma activity during adipogenesis. *International Journal of Obesity (2005), 29*(Suppl 1), S13-6.

Farmer, S. R. (2006). Transcriptional control of adipocyte formation. *Cell Metabolism, 4*(4), 263-273.

Foley, B., Clewell, R., & Deisenroth, C. (2015). Development of a human adipose-derived stem cell model for characterization of chemical modulation of adipogenesis. *Applied in Vitro Toxicology, 1*(1), 66.

Frayn, K. N., Karpe, F., Fielding, B. A., Macdonald, I. A., & Coppack, S. W. (2003). Integrative physiology of human adipose tissue. *International Journal of Obesity and Related Metabolic Disorders: Journal of the International Association for the Study of Obesity, 27*(8), 875-888.

Furuhashi, M., Saitoh, S., Shimamoto, K., & Miura, T. (2015). Fatty acid-binding protein 4 (FABP4): Pathophysiological insights and potent clinical biomarker of metabolic and cardiovascular diseases. *Clinical Medicine Insights.Cardiology, 8*(Suppl 3), 23-33.

Galic, S., Oakhill, J. S., & Steinberg, G. R. (2010). Adipose tissue as an endocrine organ. *Molecular and Cellular Endocrinology, 316*(2), 129-139.

Gerhardt, H., & Betsholtz, C. (2003). Endothelial-pericyte interactions in angiogenesis. *Cell and Tissue Research, 314*(1), 15-23.

Gimble, J. M., Bunnell, B. A., & Guilak, F. (2012). Human adipose-derived cells: An update on the transition to clinical translation. *Regenerative Medicine, 7*(2), 225-235.

Goddard, L. M., & Iruela-Arispe, M. L. (2013). Cellular and molecular regulation of vascular permeability. *Thrombosis and Haemostasis, 109*(3), 407-415.

Gomillion, C. T., & Burg, K. J. (2006). Stem cells and adipose tissue engineering. *Biomaterials, 27*(36), 6052-6063.

Goralski, K. B., McCarthy, T. C., Hanniman, E. A., Zabel, B. A., Butcher, E. C., Parlee, S. D., Muruganandan, S., & Sinal, C. J. (2007). Chemerin, a novel adipokine that regulates adipogenesis and adipocyte metabolism. *The Journal of Biological Chemistry, 282*(38), 28175-28188.

Green, H., & Kehinde, O. (1976). Spontaneous heritable changes leading to increased adipose conversion in 3T3 cells. *Cell, 7*(1), 105-113.

Green, H., & Meuth, M. (1974). An established pre-adipose cell line and its differentiation in culture. *Cell, 3*(2), 127-133.

Gregoire, F. M. (2001). Adipocyte differentiation: From fibroblast to endocrine cell. *Experimental Biology and Medicine, 226*(11), 997-1002.

Gregoire, F. M., Smas, C. M., & Sul, H. S. (1998). Understanding adipocyte differentiation. *Physiological Reviews, 78*(3), 783-809.

Gu, P., & Xu, A. (2013). Interplay between adipose tissue and blood vessels in obesity and vascular dysfunction. *Reviews in Endocrine & Metabolic Disorders, 14*(1), 49-58.

Guan, H. P., Li, Y., Jensen, M. V., Newgard, C. B., Steppan, C. M., & Lazar, M. A. (2002). A futile metabolic cycle activated in adipocytes by antidiabetic agents. *Nature Medicine, 8*(10), 1122-1128.

Hames, K. C., Koutsari, C., Santosa, S., Bush, N. C., & Jensen, M. D. (2015). Adipose tissue fatty acid storage factors: Effects of depot, sex and fat cell size. *International Journal of Obesity, 6* (Epub ahead of print).

Harms, M., & Seale, P. (2013). Brown and beige fat: Development, function and therapeutic potential. *Nature Medicine, 19*(10), 1252-1263.

Hausman, D. B., DiGirolamo, M., Bartness, T. J., Hausman, G. J., & Martin, R. J. (2001). The biology of white adipocyte proliferation. *Obesity Reviews, 2*(4), 239-254.

Hausman, G. J., & Richardson, R. L. (2004). Adipose tissue angiogenesis. *Journal of Animal Science, 82*(3), 925-934.

Holderfield, M. T., & Hughes, C. C. (2008). Crosstalk between vascular endothelial growth factor, notch, and transforming growth factor-beta in vascular morphogenesis. *Circulation Research, 102*(6), 637-652.

Huttala, O., Vuorenpaa, H., Toimela, T., Uotila, J., Kuokkanen, H., Ylikomi, T., Sarkanen, J. R., & Heinonen, T. (2015). Human vascular model with defined stimulation medium - a characterization study. *Altex, 32*(2), 125-136.

Hyvonen, M. T., & Spalding, K. L. (2014). Maintenance of white adipose tissue in man. *The International Journal of Biochemistry & Cell Biology, 56*(9), 123-132.

Iyengar, P., Espina, V., Williams, T. W., Lin, Y., Berry, D., Jelicks, L. A., Lee, H., Temple, K., Graves, R., Pollard, J., Chopra, N., Russell, R. G., Sasisekharan, R., Trock, B. J., Lippman, M., Calvert, V. S., Petricoin, E. F.,3rd, Liotta, L., Dadachova, E., Pestell, R. G., Lisanti, M. P., Bonaldo, P., & Scherer, P. E. (2005). Adipocyte-derived collagen VI affects early mammary tumor progression in vivo, demonstrating a critical interaction in the tumor/stroma microenvironment. *The Journal of Clinical Investigation, 115*(5), 1163-1176.

Jager, J., Gremeaux, T., Cormont, M., Le Marchand-Brustel, Y., & Tanti, J. F. (2007). Interleukin-1beta-induced insulin resistance in adipocytes through down-regulation of insulin receptor substrate-1 expression. *Endocrinology, 148*(1), 241-251.

Jain, R. K. (2003). Molecular regulation of vessel maturation. *Nature Medicine, 9*(6), 685-693.

Jo, J., Gavrilova, O., Pack, S., Jou, W., Mullen, S., Sumner, A. E., Cushman, S. W., & Periwal, V. (2009). Hypertrophy and/or hyperplasia: Dynamics of adipose tissue growth. *PLoS Computational Biology, 5*(3), e1000324.

Joe, A. W., Yi, L., Even, Y., Vogl, A. W., & Rossi, F. M. (2009). Depot-specific differences in adipogenic progenitor abundance and proliferative response to high-fat diet. *Stem Cells, 27*(10), 2563-2570.

Jonker, J. W., Suh, J. M., Atkins, A. R., Ahmadian, M., Li, P., Whyte, J., He, M., Juguilon, H., Yin, Y. Q., Phillips, C. T., Yu, R. T., Olefsky, J. M., Henry, R. R., Downes, M., & Evans, R. M. (2012). A PPARgamma-FGF1 axis is required for adaptive adipose remodelling and metabolic homeostasis. *Nature, 485*(7398), 391-394.

Kalluri, R. (2003). Basement membranes: Structure, assembly and role in tumour angiogenesis. *Nature Reviews.Cancer, 3*(6), 422-433.

Kang, J. H., Gimble, J. M., & Kaplan, D. L. (2009). In vitro 3D model for human vascularized adipose tissue. *Tissue Engineering.Part A, 15*(8), 2227-2236.

Kershaw, E. E., & Flier, J. S. (2004). Adipose tissue as an endocrine organ. *The Journal of Clinical Endocrinology and Metabolism, 89*(6), 2548-2556.

Kersten, S. (2014). Physiological regulation of lipoprotein lipase. *Biochimica Et Biophysica Acta, 1841*(7), 919-933.

Kokai, L. E., Marra, K., & Rubin, J. P. (2014). Adipose stem cells: Biology and clinical applications for tissue repair and regeneration. *Translational Research, 163*(4), 399-408.

Lai, M., Chandrasekera, P. C., & Barnard, N. D. (2014). You are what you eat, or are you? the challenges of translating high-fat-fed rodents to human obesity and diabetes. *Nutrition & Diabetes, 8*(4), e135.

Lanthier, N., & Leclercq, I. A. (2014). Adipose tissues as endocrine target organs. *Best Practice & Research.Clinical Gastroenterology, 28*(4), 545-558.

Lavik, E., & Langer, R. (2004). Tissue engineering: Current state and perspectives. *Applied Microbiology and Biotechnology, 65*(1), 1-8.

Lee, Y. H., Petkova, A. P., Mottillo, E. P., & Granneman, J. G. (2012). In vivo identification of bipotential adipocyte progenitors recruited by beta3-adrenoceptor activation and high-fat feeding. *Cell Metabolism, 15*(4), 480-491.

Lefterova, M. I., Haakonsson, A. K., Lazar, M. A., & Mandrup, S. (2014). PPARgamma and the global map of adipogenesis and beyond. *Trends in Endocrinology and Metabolism: TEM, 25*(6), 293-302.

Lehle, K., Straub, R. H., Morawietz, H., & Kunz-Schughart, L. A. (2010). Relevance of disease- and organ-specific endothelial cells for in vitro research. *Cell Biology International, 34*(12), 1231-1238.

LeRoith, D., & Gavrilova, O. (2006). Mouse models created to study the pathophysiology of type 2 diabetes. *The International Journal of Biochemistry & Cell Biology, 38*(5-6), 904-912.

Levenberg, S., & Langer, R. (2004). Advances in tissue engineering. *Current Topics in Developmental Biology, 61*(2), 113-134.

Lijnen, H. R. (2011). Murine models of obesity and hormonal therapy. *Thrombosis Research, 127*(Suppl 3), S17-20.

Lindroos, B., Suuronen, R., & Miettinen, S. (2011). The potential of adipose stem cells in regenerative medicine. *Stem Cell Reviews, 7*(2), 269-291.

Livak, K. J., & Schmittgen, T. D. (2001). Analysis of relative gene expression data using real-time quantitative PCR and the 2(-delta delta C(T)) method. *Methods, 25*(4), 402-408.

Lolmede, K., Durand de Saint Front, V., Galitzky, J., Lafontan, M., & Bouloumie, A. (2003). Effects of hypoxia on the expression of proangiogenic factors in differentiated 3T3-F442A

adipocytes. *International Journal of Obesity and Related Metabolic Disorders, 27*(10), 1187-1195.

Maquoi, E., Munaut, C., Colige, A., Collen, D., & Lijnen, H. R. (2002). Modulation of adipose tissue expression of murine matrix metalloproteinases and their tissue inhibitors with obesity. *Diabetes, 51*(4), 1093-1101.

Mariman, E. C., & Wang, P. (2010). Adipocyte extracellular matrix composition, dynamics and role in obesity. *Cellular and Molecular Life Sciences, 67*(8), 1277-1292.

Mead, J. R., Irvine, S. A., & Ramji, D. P. (2002). Lipoprotein lipase: Structure, function, regulation, and role in disease. *Journal of Molecular Medicine, 80*(12), 753-769.

Meissburger, B., Stachorski, L., Roder, E., Rudofsky, G., & Wolfrum, C. (2011). Tissue inhibitor of matrix metalloproteinase 1 (TIMP1) controls adipogenesis in obesity in mice and in humans. *Diabetologia, 54*(6), 1468-1479.

Morris, A. W., Carare, R. O., Schreiber, S., & Hawkes, C. A. (2014). The cerebrovascular basement membrane: Role in the clearance of beta-amyloid and cerebral amyloid angiopathy. *Frontiers in Aging Neuroscience, 19*(6), 251.

Ntambi, J. M., & Young-Cheul, K. (2000). Adipocyte differentiation and gene expression. *The Journal of Nutrition, 130*(12), 3122S-3126S.

Ong, W. K., & Sugii, S. (2013). Adipose-derived stem cells: Fatty potentials for therapy. *The International Journal of Biochemistry & Cell Biology, 45*(6), 1083-1086.

Pasarica, M., Sereda, O. R., Redman, L. M., Albarado, D. C., Hymel, D. T., Roan, L. E., Rood, J. C., Burk, D. H., & Smith, S. R. (2009). Reduced adipose tissue oxygenation in human obesity: Evidence for rarefaction, macrophage chemotaxis, and inflammation without an angiogenic response. *Diabetes, 58*(3), 718-725.

Patrick, C. W.,Jr. (2001). Tissue engineering strategies for adipose tissue repair. *The Anatomical Record, 263*(4), 361-366.

Peirce, V., Carobbio, S., & Vidal-Puig, A. (2014). The different shades of fat. *Nature, 510*(7503), 76-83.

Poulos, S. P., Hausman, D. B., & Hausman, G. J. (2010). The development and endocrine functions of adipose tissue. *Molecular and Cellular Endocrinology, 323*(1), 20-34.

Rasouli, N., & Kern, P. A. (2008). Adipocytokines and the metabolic complications of obesity. *The Journal of Clinical Endocrinology and Metabolism, 93*(Suppl 1), S64-73.

Ries, C. (2014). Cytokine functions of TIMP-1. *Cellular and Molecular Life Sciences, 71*(4), 659-672.

Risau, W. (1998). Development and differentiation of endothelium. *Kidney International.Supplement, 67*(Suppl 10), S3-6.

Ronti, T., Lupattelli, G., & Mannarino, E. (2006). The endocrine function of adipose tissue: An update. *Clinical Endocrinology, 64*(4), 355-365.

Rosen, E. D., & MacDougald, O. A. (2006). Adipocyte differentiation from the inside out. *Nature Reviews.Molecular Cell Biology, 7*(12), 885-896.

Rosen, E. D., & Spiegelman, B. M. (2014). What we talk about when we talk about fat. *Cell, 156*(1-2), 20-44.

Roy, S., Maiello, M., & Lorenzi, M. (1994). Increased expression of basement membrane collagen in human diabetic retinopathy. *The Journal of Clinical Investigation, 93*(1), 438-442.

Rupnick, M. A., Panigrahy, D., Zhang, C. Y., Dallabrida, S. M., Lowell, B. B., Langer, R., & Folkman, M. J. (2002). Adipose tissue mass can be regulated through the vasculature. *Proceedings of the National Academy of Sciences of the United States of America, 99*(16), 10730-10735.

Rutkowski, J. M., Stern, J. H., & Scherer, P. E. (2015). The cell biology of fat expansion. *The Journal of Cell Biology, 208*(5), 501-512.

Sade, R. M. (2011). From laboratory to bedside: Ethical, legal and social issues in translational research. *The American Journal of the Medical Sciences, 342*(4), 265-266.

Saiki, A., Watanabe, F., Murano, T., Miyashita, Y., & Shirai, K. (2006). Hepatocyte growth factor secreted by cultured adipocytes promotes tube formation of vascular endothelial cells in vitro. *International Journal of Obesity, 30*(11), 1676-1684.

Sarkanen, J. R., Kaila, V., Mannerstrom, B., Raty, S., Kuokkanen, H., Miettinen, S., & Ylikomi, T. (2012a). Human adipose tissue extract induces angiogenesis and adipogenesis in vitro. *Tissue Engineering.Part A, 18*(1-2), 17-25.

Sarkanen, J. R., Vuorenpaa, H., Huttala, O., Mannerstrom, B., Kuokkanen, H., Miettinen, S., Heinonen, T., & Ylikomi, T. (2012b). Adipose stromal cell tubule network model provides a versatile tool for vascular research and tissue engineering. *Cells, Tissues, Organs, 196*(5), 385-397.

Sarkar, S., & Schmued, L. (2012). In vivo administration of fluorescent dextrans for the specific and sensitive localization of brain vascular pericytes and their characterization in normal and neurotoxin exposed brains. *Neurotoxicology, 33*(3), 436-443.

Scherer, P. E. (2006). Adipose tissue: From lipid storage compartment to endocrine organ. *Diabetes, 55*(6), 1537-1545.

Scroyen, I., Hemmeryckx, B., & Lijnen, H. R. (2013). From mice to men--mouse models in obesity research: What can we learn? *Thrombosis and Haemostasis, 110*(4), 634-640.

Selvarajan, S., Lund, L. R., Takeuchi, T., Craik, C. S., & Werb, Z. (2001). A plasma kallikrein-dependent plasminogen cascade required for adipocyte differentiation. *Nature Cell Biology, 3*(3), 267-275.

Senger, D. R., & Davis, G. E. (2011). Angiogenesis. *Cold Spring Harbor Perspectives in Biology, 3*(8), a005090.

Spalding, K. L., Arner, E., Westermark, P. O., Bernard, S., Buchholz, B. A., Bergmann, O., Blomqvist, L., Hoffstedt, J., Naslund, E., Britton, T., Concha, H., Hassan, M., Ryden, M., Frisen, J., & Arner, P. (2008). Dynamics of fat cell turnover in humans. *Nature, 453*(7196), 783-787.

Stapor, P. C., Sweat, R. S., Dashti, D. C., Betancourt, A. M., & Murfee, W. L. (2014). Pericyte dynamics during angiogenesis: New insights from new identities. *Journal of Vascular Research, 51*(3), 163-174.

Sun, K., Kusminski, C. M., & Scherer, P. E. (2011). Adipose tissue remodeling and obesity. *The Journal of Clinical Investigation, 121*(6), 2094-2101.

Switzer, N. J., Mangat, H. S., & Karmali, S. (2013). Current trends in obesity: Body composition assessment, weight regulation, and emerging techniques in managing severe obesity. *Journal of Interventional Gastroenterology, 3*(1), 34-36.

Szoke, K., Beckstrom, K. J., & Brinchmann, J. E. (2012). Human adipose tissue as a source of cells with angiogenic potential. *Cell Transplantation, 21*(1), 235-250.

Thalmann, S., & Meier, C. A. (2007). Local adipose tissue depots as cardiovascular risk factors. *Cardiovascular Research, 75*(4), 690-701.

Tran, K. V., Gealekman, O., Frontini, A., Zingaretti, M. C., Morroni, M., Giordano, A., Smorlesi, A., Perugini, J., De Matteis, R., Sbarbati, A., Corvera, S., & Cinti, S. (2012). The vascular endothelium of the adipose tissue gives rise to both white and brown fat cells. *Cell Metabolism, 15*(2), 222-229.

Trayhurn, P. (2013). Hypoxia and adipose tissue function and dysfunction in obesity. *Physiological Reviews, 93*(1), 1-21.

Tsuji, W., Rubin, J. P., & Marra, K. G. (2014). Adipose-derived stem cells: Implications in tissue regeneration. *World Journal of Stem Cells, 6*(3), 312-321.

Ucuzian, A. A., & Greisler, H. P. (2007). In vitro models of angiogenesis. *World Journal of Surgery, 31*(4), 654-663.

van Baak, M. A. (2013). Nutrition as a link between obesity and cardiovascular disease: How can we stop the obesity epidemic? *Thrombosis and Haemostasis, 110*(4), 689-696.

Verseijden, F., Jahr, H., Posthumus-van Sluijs, S. J., Ten Hagen, T. L., Hovius, S. E., Seynhaeve, A. L., van Neck, J. W., van Osch, G. J., & Hofer, S. O. (2009). Angiogenic capacity of human adipose-derived stromal cells during adipogenic differentiation: An in vitro study. *Tissue Engineering.Part A, 15*(2), 445-452.

Vestweber, D. (2008). VE-cadherin: The major endothelial adhesion molecule controlling cellular junctions and blood vessel formation. *Arteriosclerosis, Thrombosis, and Vascular Biology, 28*(2), 223-232.

Viguerie, N., Montastier, E., Maoret, J. J., Roussel, B., Combes, M., Valle, C., Villa-Vialaneix, N., Iacovoni, J. S., Martinez, J. A., Holst, C., Astrup, A., Vidal, H., Clement, K., Hager, J., Saris, W. H., & Langin, D. (2012). Determinants of human adipose tissue gene expression: Impact of diet, sex, metabolic status, and cis genetic regulation. *PLoS Genetics, 8*(9), e1002959.

Walther, T. C., & Farese, R. V.,Jr. (2012). Lipid droplets and cellular lipid metabolism. *Annual Review of Biochemistry, 81*, 687-714.

Wang, P., Mariman, E., Renes, J., & Keijer, J. (2008). The secretory function of adipocytes in the physiology of white adipose tissue. *Journal of Cellular Physiology, 216*(1), 3-13.

Wang, Q. A., Scherer, P. E., & Gupta, R. K. (2014). Improved methodologies for the study of adipose biology: Insights gained and opportunities ahead. *Journal of Lipid Research, 55*(4), 605-624.

Watson, R. T., & Pessin, J. E. (2007). GLUT4 translocation: The last 200 nanometers. *Cellular Signalling, 19*(11), 2209-2217.

Weisberg, S. P., McCann, D., Desai, M., Rosenbaum, M., Leibel, R. L., & Ferrante, A. W.,Jr. (2003). Obesity is associated with macrophage accumulation in adipose tissue. *The Journal of Clinical Investigation, 112*(12), 1796-1808.

Wittmann, K., Dietl, S., Ludwig, N., Berberich, O., Hoefner, C., Storck, K., Blunk, T., & Bauer-Kreisel, P. (2015). Engineering vascularized adipose tissue using the stromal-vascular fraction and fibrin hydrogels. *Tissue Engineering.Part A, 21*(7-8), 1343-1353.

Yen, C. L., Stone, S. J., Koliwad, S., Harris, C., & Farese, R. V.,Jr. (2008). Thematic review series: Glycerolipids. DGAT enzymes and triacylglycerol biosynthesis. *Journal of Lipid Research, 49*(11), 2283-2301.

Zechner, R., Strauss, J. G., Haemmerle, G., Lass, A., & Zimmermann, R. (2005). Lipolysis: Pathway under construction. *Current Opinion in Lipidology, 16*(3), 333-340.

Appendices

Appendix 1: Used hASC-HUVEC combinations in different experiments

Experiment 1: hASC153+HUVEC20

Experiment 2: hASC29+HUVEC25

Experiment 3: hASC161+HUVEC19

Experiment 4: hASC161+HUVEC19

Experiment 5: hASC29+HUVEC25

Experiment 6: hASC161+HUVEC19

Experiment 7: hASC153+HUVEC20

Appendix 2: Used ATE batches in different experiments

Experiment 1: Pool: 10 % ATE153, 60 % ATE159, 30 % ATE162

Experiment 2: ATE187 (first two exposures), ATE177 (last two exposures)

Experiment 3: ATE183

Experiment 4: ATE159

Experiment 5: ATE177

Experiment 6: Pool: 50 % ATE159, 50 % ATE 183

Experiment 7: Pool: 50 % ATE177, 25% ATE183, 25% ATE159